QUALITY-CENTRIC AUTHENTICATION OF ADDITIVELY MANUFACTURED PARTS THROUGH VORONOI-BASED ERROR EXAGGERATION

A Thesis

by

RIDDHI RAMESH ADHIKARI

Submitted to the Graduate and Professional School of
Texas A&M University
in partial fulfillment of the requirements for the degree of

MASTER OF SCIENCE

Chair of Committee,	Vinayak R. Krishnamurthy
Committee Members,	Ergun Akleman
	Bruce L. Tai
Head of Department,	Bryan P. Rasmussen

December 2021

Major Subject: Mechanical Engineering

ABSTRACT

Additive manufacturing or rapid prototyping is continuously gaining popularity within and outside the research community. Due to its growing applications and technical and economical advantages over conventional machining, additive manufacturing is being used even to manufacture critical components in aerospace and automobile industry. As a result, there is also an increase in counterfeiting in this technology which can pose a threat to proprietary parts.

This research work deals with authenticating 3D printed parts by comparing the quality of the parts with the precision and bias of 3D printers. The idea is to be able to differentiate between the error distributions of two printers so as to authenticate the parts printed on them. Therefore, the primary research goal of this work is to be able to quantify the differences in error distributions across different printers and characterization of printers. The key challenge is that it is difficult to robustly quantify the difference between two printers simply by comparing their coordinate error distributions. To address this challenge, we introduce a novel topological transformation based on the principle of Voronoi Tessellation, called *SplitCode*, that exaggerates the differences in coordinate error distributions, thereby, enabling us to better differentiate two given printers quantitatively. Consequently, the method leads to a robust authentication of 3D printed parts.

In this work, through numerical simulations we study the effect of varying mean and standard deviation of error distributions on topological transformation. We find out that maximum exaggeration of the difference between error distributions is achieved on using length, angle and midpoint location to represent the split edge. We present a methodology for quality assessment and authentication and study the effect of different known distributions on authentication. On validating our scheme numerically, we learn that application of *SplitCode* improves accuracy of authentication between printers with same bias but different precision.

Finally, experimental results show that authentication is possible between two printers with different biases both before and after application of *SplitCode*. However, authentication of lower quality parts printed on the same printer but at different speeds is influenced by the nature of error

distributions of the printer and the print. In certain cases, application of *SplitCode* is required for authenticating prints that have same bias but different precision. The results of both simulated and experimental studies show that when the quality of the part changes and the problem is to identify a lower quality part, application of *SplitCode* results in better authentication. This highlights the quality-centric approach of authentication. This research work also offers various opportunities of further exploration in terms of part design, algorithm of *SplitCode*, imaging and post processing methods and statistical variations.

DEDICATION

To my mother *Rajashree*,

For always encouraging me and loving me unconditionally.

To my father *Ramesh*,

For supporting me with the choices I have made.

To my family and friends,

For holding me up during times when goals seemed unattainable.

ACKNOWLEDGMENTS

After one unsupervised semester at Texas A&M University, I joined the Mixed Initiative Design Lab under Dr. Krishnamurthy in January 2020. And since then I have been on a journey of fascinating experiences. I am extremely grateful to Dr. Krishnamurthy for his unbounded support and guidance during this time. Since the time I started doing research under him, he has been personally involved in everything related to my research. There has not been a time when I had reached a dead end and he did not have a solution to it. This would not have been possible if it wasn't for his hands on style and never exhausting enthusiasm. I am truly thankful for everything I have experienced in the lab under his guidance in these two years.

My other constant source of inspiration is Dr. Akleman. His zest has always motivated me to learn more and do more. He has always supplied me with beautiful ideas and helped me to understand its beauty. I consider myself fortunate for being able to be on the receiving end of his vast knowledge and wisdom. Special thanks to Dr. Panchal for collaborating with us in this research work. Throughout this research work, his valuable advice has proved to be of great significance in steering this work in the right direction. I also want to thank Dr. Tai for supporting this research in every possible way.

Next, I would like to thank student collaborators Karim and Adam, who helped me in printing shapes and generating data from the images of the prints. I would also like to thank Ronak and Sai Ganesh for motivating me in my initial few days at the lab and helping me in kick-starting my work. I want to thank all my lab-mates - Matt, Shantanu, Abhijeet and Subhrajyoti for being so understanding and supportive. I am also grateful for my friends - Sejal, Kavit, Anagha, Kavan and Malliga who were there for me in all difficult times when family could not be here. Thanks to Sharat Chandra who has been with me on this roller coaster and taken care of me when I couldn't. Finally, I have been blessed to have a family who is so supportive and encouraging all the time. I want to take this opportunity to thank my mother, father, brother and sister-in-law for every single thing in my life. They have always shown their trust in me and I hope I have made them proud.

CONTRIBUTORS AND FUNDING SOURCES

Contributors

This work was supported by a thesis committee consisting of Dr. Vinayak R. Krishnamurthy and Dr. Bruce L. Tai of the Department of Mechanical Engineering and Dr. Ergun Akleman of the Department of Architecture and Visualization. This work was also supervised by Dr. Jitesh Panchal of School of Mechanical Engineering, Purdue University.

The printed parts and image data of the parts analyzed in Chapter IV were provided by students Karim A. ElSayed and Adam Dachowicz of School of Mechanical Engineering, Purdue University.

All other work conducted for the thesis was completed by the student independently.

Funding Sources

The graduate student was supported through a Graduate Research Assistantship by the Texas A&M University and Department of Mechanical Engineering.

NOMENCLATURE

OGAPS	Office of Graduate and Professional Studies at Texas A&M University
TAMU	Texas A&M University
AM	Additive Manufacturing
FDM	Fused Deposition Modelling
CAD	Computer-Aided Design
G Code	Geometric Code
3D	Three Dimensional
2D	Two Dimensional
RGB	Red Green Blue
KL	Kullback–Leibler
KS	Kolmogorov–Smirnov

TABLE OF CONTENTS

Page

LIST OF FIGURES

FIGURE Page

1. INTRODUCTION

As Campbell et al. highlight in their work, *"Additive Manufacturing is perhaps at the point of the earliest development of personal computers or at the beginnings of the Internet and World Wide Web"* [1]. The first 3D printer was developed by Charles W. Hull of 3D Systems Corporation in 1984. At that time, 3D printers were either very expensive and offered high capabilities or they were designed to do the ordinary at a lower price [2]. Therefore, it was not until recently that the cost associated with 3D printing reduced to the extent that a wide variety of industries adopted it [3, 4]. Many industries including aerospace[5, 6, 7], automotive[8] and medical industry [9, 10, 11] welcomed additive manufacturing (AM) because of its ability to produce faster with more accuracy and at lower cost [12]. Currently, AM is being used to produce critical components in these industries [1]. Because of the advantages offered by this technology, it is expected to grow more than double the size in the next five years [13].

As the range of applications of 3D printing is widening [14], it is natural to expect threats such as theft of technical data, counterfeiting, sabotage for additively manufactured parts [15]. These attacks have the potential to cause economic losses to both small and large businesses. In order to prevent this, authentication of additively manufactured parts is of critical significance. In this thesis, we introduce a quality-centric authentication method to prevent counterfeiting at the manufacturing level.

Our approach is based on the principle of exaggeration of the coordinate errors that is (1) present in all 3D printers and (2) is usually different across printers. We characterize 3D printers by characterizing the precision and bias of the printers. Precision and bias of a printer can be estimated from the error in the part printed by the printer with respect to its CAD model. However, it might not be always possible to differentiate between two printers by directly comparing their error distributions because of inconsequential distinction between the two printers. To address this challenge, we propose a novel technique called '*SplitCode*' that topologically transforms the error distributions of printers by application of Voronoi tessellations and exaggerates the difference

between two printers. This allows us to assess the quality of the parts and compare it with the error distributions of printers. Consequently, this method enables us to achieve better authentication for additively manufactured parts.

1.1 Additive Manufacturing and its Advantages

Additive manufacturing (AM) is a process of manufacturing three dimensional objects in a layer-by-layer fashion based on a CAD model [16], [17]. Over the years multiple techniques of AM came into existence. Some of the most commonly used techniques are stereolithography, selective laser sintering and fused deposition modeling technique [2]. Although AM cannot completely replace conventional manufacturing processes, it has several advantages over it[15].

AM processes involves less time and cost penalties [17] and the required startup cost is also less as compared to conventional machines. There are fewer restrictions on the design and we could produce any complex shape that could be very difficult to machine [2]. Just - in - time and on - demand production is also possible as manufacturing lead times are reduced [16]. Thus, AM helps new designs to reach market quickly. This technology also enables mass customization without involving much cost and time [18]. Overall, AM could be very useful for manufacturing some complex parts with just little human intervention. Due to several technical and economic advantages, AM has gained popularity in the past and continues to grow further.

1.2 Applications of Additive Manufacturing

AM is being used in major industries such as aerospace, automotive, and medical industry for producing critical components. AM has enabled production of light weight structures in both the aerospace and automotive industry [17]. Space X used additively manufactured engine chambers in the Dragon spacecraft [19, 20]. General electric also made 3D printed structural parts that weighed 80% lighter than conventional parts [21]. NASA first used fused deposition modelling to create support structures in their COSMIC-2 (Constellation Observing System for Meteorology, Ionosphere, and Climate-2) mission that were exposed to the space environment [22]. Later they continued testing of AM in zero gravity environment to be able to provide on-demand manufactur-

Figure 1.1: Applications of Additive Manufacturing Process in aerospace, automotive and medical industry.

ing for astronauts [2].

AM is a great attraction in automotive industry as it can be used for communicating and validating design through prototyping [23]. It can also be used to produce manufacturing tools and jigs, fixtures [24]. However, it is not just used for prototyping but also for producing functional components and reproducing difficult to find components[25]. Some of the applications of 3D printing in the medical industry are bio-printing of tissues and organs, making customized implants and prostheses and creating anatomical models for surgical preparations [26, 27]. 3D printing also provides creative opportunities in architecture like building from recyclable materials[28]. Thus, AM has a wide range of critical applications and the market is still growing[29].

1.3 Security Issues in Additive Manufacturing

Increasing demand for AM has led to an increase in the security risks associated with AM. While these may not affect educational and prototyping applications of AM, they pose a serious threat to domains where the failure of even a small part may cause severe loss of profits (and in some cases, life).[16]

As such, there are several possible ways of introducing security risks in the AM process. Potential ways in which that be achieved is by stealing design or printing data, and sabotaging. Not only that, these risks can be introduced at multiple steps in the AM process including designing, slicing, and printing. AM is a multi step process combining both automated and manual workflows. The process begins with designing a computer-aided model of the part to be printed and storing

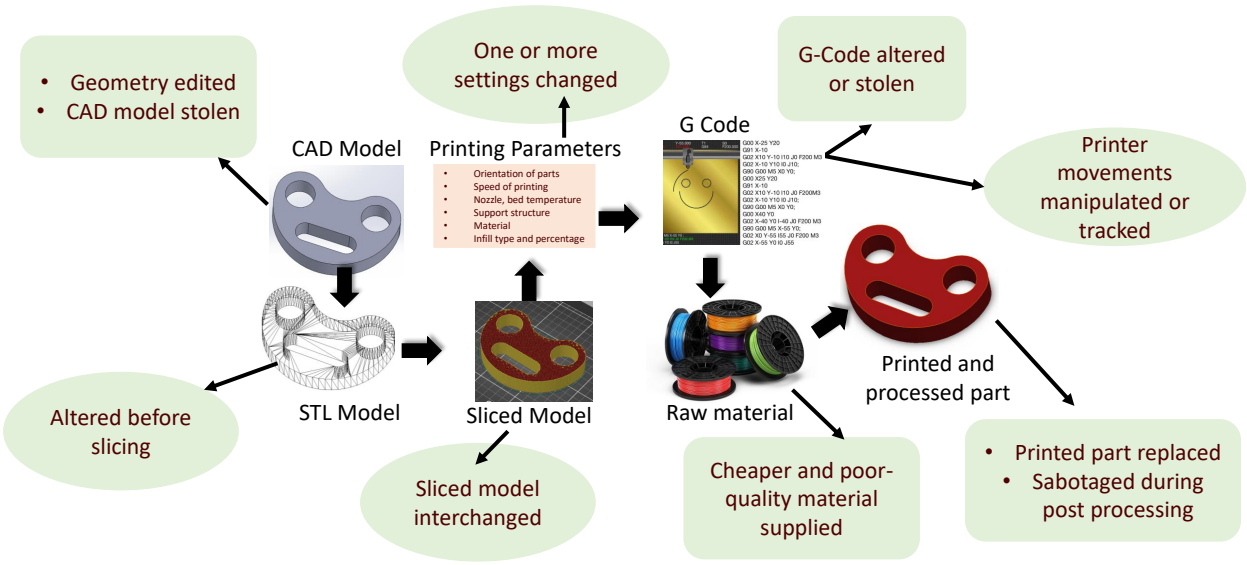

Figure 1.2: Potential attacks in the Additive Manufacturing Process.

design in a format that is compatible with 3D printers, such as STereoLithography(STL), Additive Manufacturing File(AMF) and 3D Manufacturing Format(3MF). This design is then sliced in a slicer software into multiple layers that can be printed. At this time other parameters of printing like the speed, infill type, infill percentage, material and temperature are also selected according to requirement. This information is then used to create a G Code with commands to control the position of the printing nozzle and the bed. Simultaneously, printing material is fed in the printer to prepare it for printing and the printing is started. After printing, the part is post processed to get a finished product. Yampolskiy et al. and Chen et al. [16, 21, 30], discussed in their work about how any one or multiple of these elements in this process could be compromised and manipulated to cause a threat to the end product.

At the very beginning of the process, CAD model could be stolen or the design could be edited resulting in either faulty end product or counterfeiting [31]. The slicer software could be bugged to change the settings of printing resulting in poor quality parts. Then the G Code could be altered to control the printer movement or the printer could be attacked. Printer movement could also be tracked and reproduced to manufacture fake parts. Material of printing could be replaced by

a lower quality material. And lastly, the finished part could be sabotaged or used for reverse engineering a lower quality and cheaper part. These attacks are categorized in two main groups - theft of technical data[30, 32, 33, 34] and sabotage [16, 35, 31, 36]. Theft of technical data gives rise to counterfeiting in this technology resulting in lower quality end products.

1.4 Counterfeiting in Additive Manufacturing

Counterfeiting aids production of sub-quality end products. Counterfeiting can occur at various levels in the 3D printing process [37, 38]. It can take place at the designer level where counterfeiter acquires access to the authentic CAD model and uses it to manufacture a spurious part [39]. Or it can take place at the manufacturing level where the manufacturer prints the authentic CAD model on an unauthentic printer or on the authentic printer at higher speeds. Both these cases result in end products which are of lower standard in terms of precision and quality as compared to the authentic parts. This eventually leads to failure of additively manufactured parts, economic losses and endangered human lives. Even aerospace, automotive and medical industries have suffered great losses due to counterfeiting[40]. Hence, it is important to identify attempts of counterfeiting and minimize the losses caused by it. Researchers have extensively explored this problem and introduced several authentication methods.

1.5 Authentication methods in Additive Manufacturing

Some of the existing authentication methods utilize external appearance of printed parts for surface tagging while others take advantage of the inner structure. Technique proposed by Harrison et al. [41] is an example of the former. They presented barcodes in the form of physical notches on the surface of the printed part. When the barcodes are swiped by fingernails, they produce specific sound waves. These sound waves are later used for authenticating parts. However, such methods affect the appearance of the 3D printed parts [42].

Later Gupta et al. [43] proposed a method of introducing additional features in the internal structure of the printed parts. Because of these features the quality of the part is maintained only when specific printing conditions are met and in all other cases quality degrades. The disadvantage

of this method is that poor quality of 3D printed parts cannot be measured directly. It can only be detected when the part fails prematurely. On the other hand, Chen et al. [44, 45, 46], discussed embedding of QR codes in the part by diving the code into multiple layers. This helped to eliminate the effect of additional features on the mechanical properties of the 3D printed part. This methods could only be applied to part with high infill percentage and also demanded designing of each part individually.

For authentication in lower filled part, Kubo et al. [47] presented a method of using resonant properties of objects. In this method, 3D printed parts are assigned unique resonant properties by changing their internal structure. The change in the internal structure is captured with acoustic sensing. This can be used to differentiate parts even if they have same external appearance. They later extended their work by using printing conditions directly to create unique resonant properties which reduced the effort of 3D modeling every part separately[48].

In 2018, Li et al. made an important argument [49] that 3D printers possess unique fingerprints resulting from its hardware imperfections. In their work, they modelled a connection between the fingerprints and the texture on the 3D printed parts. Similarly, Dogan et al.[50] utilized the patterns appearing on the 3D printed objects due to slicing instead of adding extra features to the part for authentication. The patterns appear to be varying with varying slicing parameters. Some authentication methods involve complex designing or require use of advanced technology [51, 52]. This limits their application in everyday situation [50]. Taking inspiration from these works, we propose a method called *SplitCode* to address some of the existing challenges.

1.6 Overview of *SplitCode*

In order to identify if a 3D printed part is printed on a given 3D printer, our approach is to compare the quality of the part with the precision and bias of the 3D printer. To quantify the quality of a given part we measure the positional errors in the part with respect to the ground truth, that is its ideal CAD model. Due to mechanical imperfections of the printer, there will be some error in the part printed by the printer. Positional errors measured in multiple parts printed on a given printer generates a reference error distribution for that printer. This error distribution

is unique to every printer as it is indicative of the precision and bias of that particular printer. The overarching idea is to differentiate between error distributions of two printers so as to be able to determine if the positional errors in a given printed part come from the same distribution as that of the reference printer's error distribution. However, it might not always be possible to quantify the difference between two error distributions. Hence, we first want to exaggerate the difference between coordinate error distributions of two printers. Our approach to deal with this is based on the principle of Voronoi Tessellation as it offers a method to achieve this exaggeration by exaggerating the coordinate errors present in 3D printers.

1.7 Overview of Thesis

The thesis is organized into four main parts. In Chapter 2, we introduce a novel topological transformation technique called *SplitCode*. We start by describing the algorithm of *SplitCode* in detail and see how using this technique we can exaggerate the difference in error distributions of two printers and characterize printers. We then discuss the design of scheme. We present a systematic study for selecting the most useful representation of the split edge that gives us maximum exaggeration between two error distributions. In Chapter 3, we propose a methodology for quality assessment and authentication of additively manufactured parts. We also validate our theory numerically and study the effect of different known distributions on authentication. We see how to apply our method to real applications through some physical experiments in Chapter 4. Finally, in Chapter 5, we summarize our contributions and discuss some of the future implications of this research work.

2. *SPLITCODE*: Algorithm and Design of Scheme

2.1 Introduction

Our approach for assessing the quality of print and authenticating a given print is based on comparing topological noise of printers. Each printer carries some inherent characteristics resulting from its mechanical components such as motors and nozzles. These characteristics are unique to every printer. Whenever any part is printed on the printer, the printer characteristics are passed on to the printed part in the form of errors or deviations. Thus, each part printed by a printer carries a unique fingerprint associated with that printer.

Usually, while embedding information in 3d printed parts, the attempt is to either minimize the errors in printing or to introduce additional controlled errors. In our work, instead of trying to eliminate these errors or introduce new errors, we utilize the existing coordinate error distribution of printers for identifying if a given test print is printed on the given printer. In order to do this, first task is to obtain coordinate error distributions of the printer and the test print.

2.2 Generation of Error Distributions of Printer and Test Print

Coordinate error distribution denotes the error in the location of features printed by the printer with respect to their ideal CAD locations. This error is representative of both bias and precision of the printer. As shown in Figure 2.1, to generate error distributions we start with a part design consisting of some features where error can be measured. Here, we design a part with circular

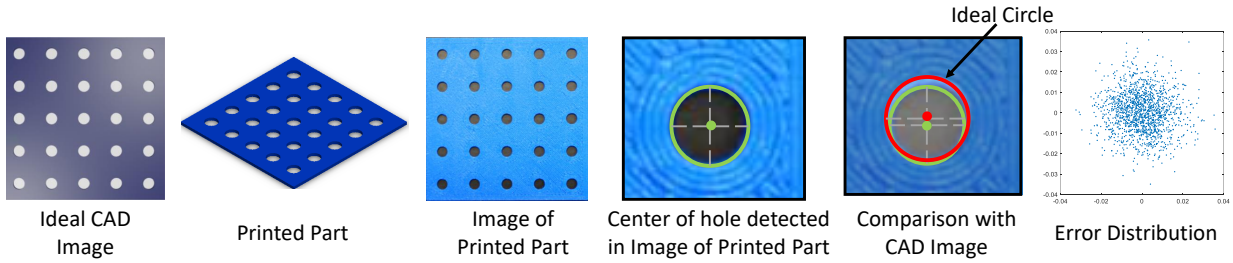

Figure 2.1: Generation of error distribution of a printed part.

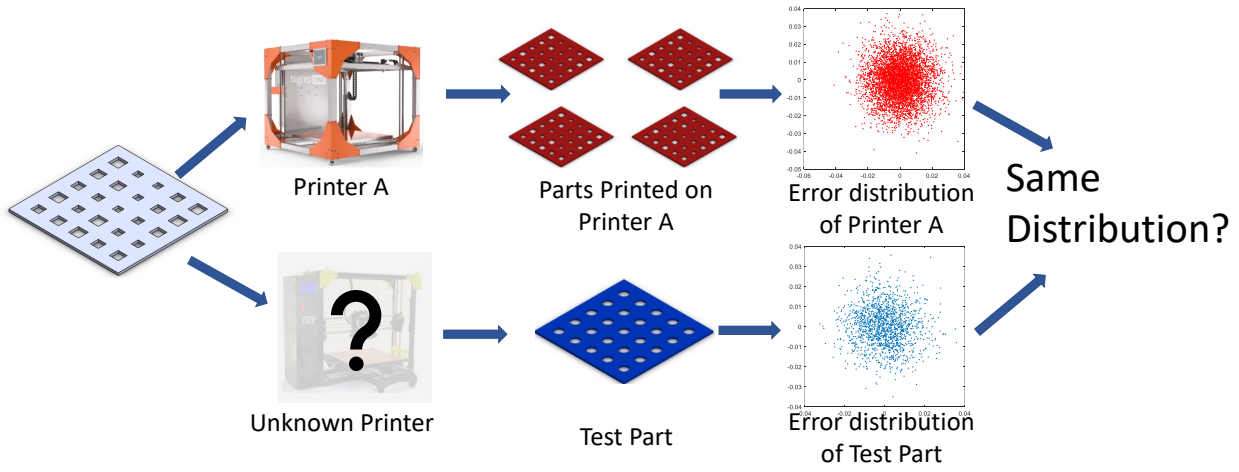

Figure 2.2: To find if the test print is printed on the reference printer, we compare the printer's reference error distribution and the test error distribution to see if they belong to the same distribution.

holes. We then print this design and take multiple images of the print. Our next job is register the image of the CAD model on the captured images of the print and detect the centers of the circles in both the images. Because of the noise in printer there will be some error between the centers of the holes detected in the print and the centers of the holes in the ideal CAD image. Error generated while printing multiple such holes gives us the error distribution of that print. Here, circular holes and the centers are just an example of the features that can be used to measure error. We can substitute them with other features like corners of square holes.

When multiple prints of this CAD design are printed on a given printer (p_A), these prints act as the reference prints of the printer. Error measured in all the prints contribute to the reference error distribution of the printer (p_A). Therefore, coordinate error distribution of any printer can be achieved as we compute errors in multiple parts printed by the printer and compare it with the ideal CAD image of the part. Similarly, if we have a test print (t_A) printed on an unknown printer, error measured in the test print gives us the test error distribution.

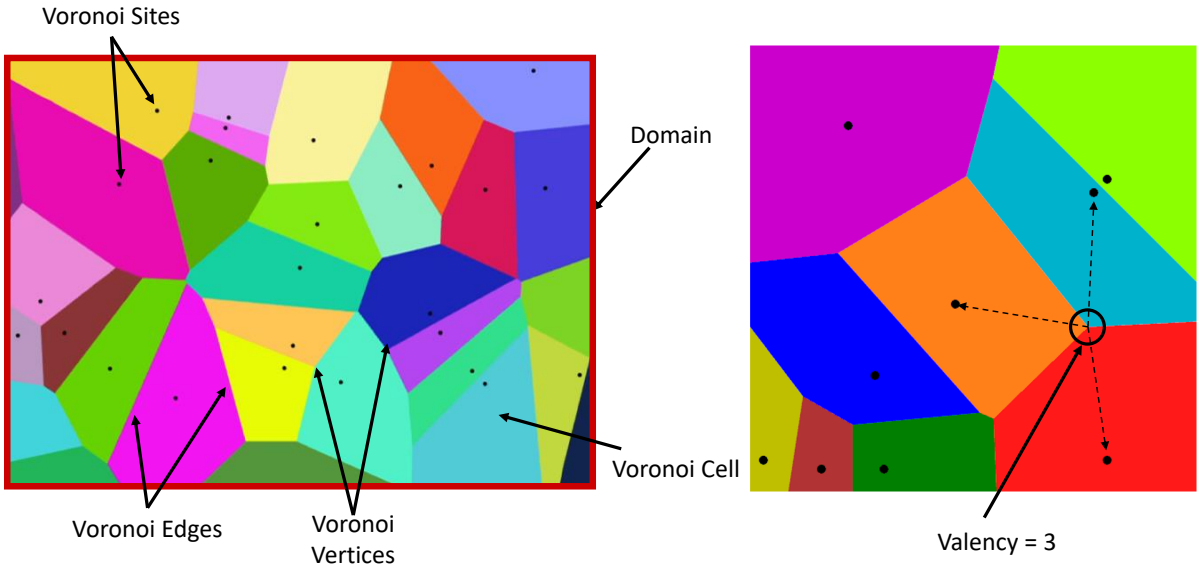

Figure 2.3: Voronoi Tessellation.

2.3 Broader Goals and Challenges

If we want to find out whether the test print (t_A) is printed on the reference printer (p_A) or not, we need to determine if the reference error distribution of the printer and the test error distribution belong to the same distribution. So the primary research goal is to first be able to quantify the difference between error distributions of two printers and characterize the printers. The idea is that if we are able to differentiate between two printers i.e. differentiate between error distributions of two printers, we would also be able to authenticate parts printed on the two printers.

The key challenge here is that error distributions of some printers could be similar to each other and it is difficult to differentiate between them just by comparing them with each other. To address this challenge, we first aim to exaggerate the differences between two error distributions. Here, we make a critical observation that Voronoi tessellation can be effectively used for this purpose as it offers a method to achieve this exaggeration.

2.4 Voronoi Tessellations

Voronoi tessellation or Voronoi diagram (Figure 2.3) [53, 54] is the result that we get when a 2D space is decomposed into smaller regions based on some seed points, such that every point in

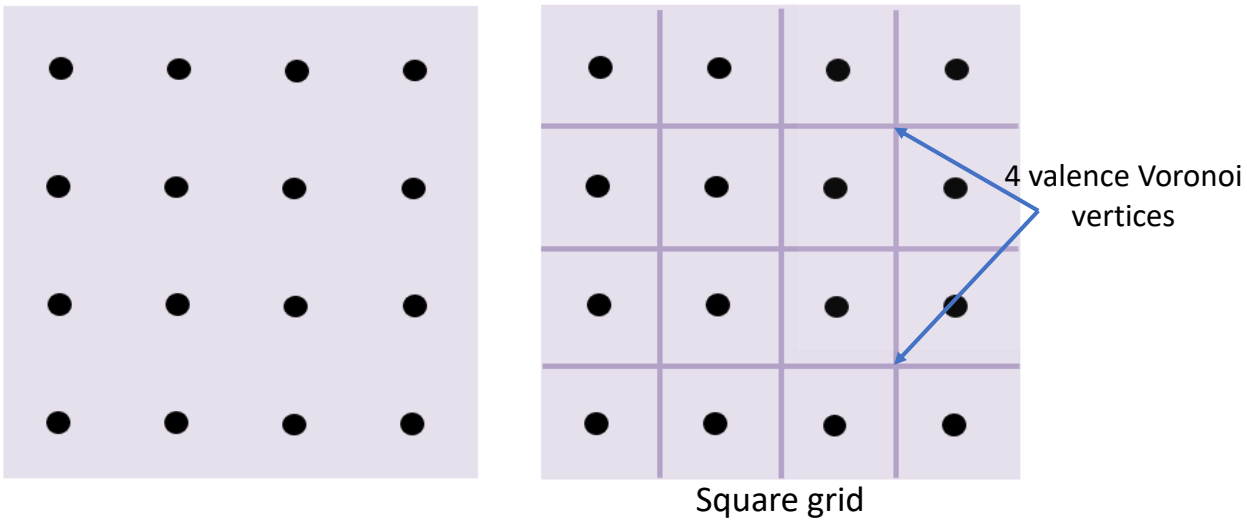

Figure 2.4: Grid of Voronoi sites generating a grid of quad cells.

a given region is closest to its corresponding seed point in that region. In the Voronoi diagram, 2D space is called the domain, seed points are known as Voronoi sites and the small regions are called Voronoi cells. Two other features of the Voronoi diagram are the straight line boundaries of the Voronoi cells known as Voronoi edges and the points where the edges meet each other called the Voronoi vertices. An important characteristic associated with Voronoi vertices is their valency. For example, when three edges are incident on a vertex, the valency of the vertex is three and when four edges are incident on it, the valency is four.

2.5 Topology Change in the Voronoi Diagram

When Voronoi sites in a given Voronoi diagram start moving, naturally the shape of the Voronoi cells change, but in addition to that, change in topology also occurs. Some of the Voronoi edges in the diagram collapse into four valence vertices and then again the four valence vertices split into edges. This concept is called vertex splitting. The topology change occurring in the Voronoi diagram due to change in the location of the sites is the reason why we consider Voronoi Tessellation as the solution for achieving exaggeration between two error distributions.

If we consider a grid of Voronoi sites in a 2D domain and compute their Voronoi diagram, we get a grid of quad cells where all vertices have valency four as shown in Figure 2.4. Now when

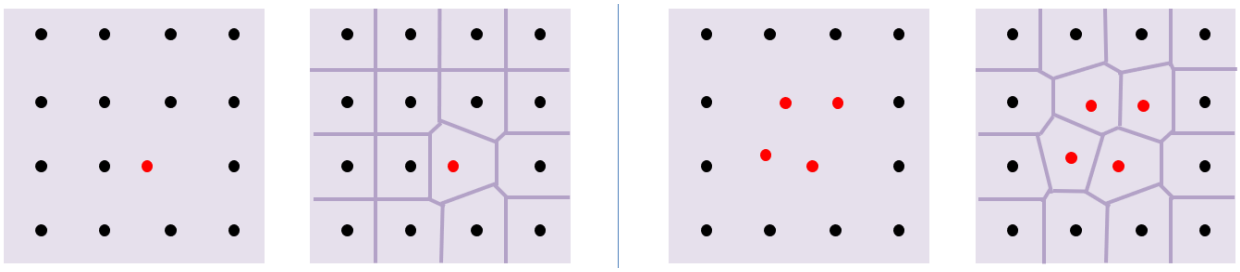

Figure 2.5: Change in topology occurring as four valence vertices split into Voronoi edges.

we move either one or more of these sites from their original location in the grid and compute their Voronoi diagram, we do not get a grid of quad cells (Figure 2.5). As the Voronoi sites are no longer arranged in a grid, four valence vertices split into edges. This means that Voronoi diagram is sensitive to even minor changes in the arrangement of Voronoi sites and these minor changes are exaggerated through change in topology. Hence, we use Voronoi tessellation for topological transformation of coordinate error distribution of printers and printed parts.

2.6 Algorithm

The first step towards characterization of printers is topological transformation of their coordinate error distributions. In order to do so, we go through the following steps:

Step 1. We start with four points arranged along the vertices of a square inside a bigger square of same orientation. The four points act as Voronoi sites and the bigger square serves as the domain for Voronoi computation.

Step 2. We divide the domain into four Voronoi cells by computing Voronoi diagram for the four Voronoi sites. Since the Voronoi sites are arranged along the vertices of a square, the resulting Voronoi cells are also squares giving us a grid of quad cells. The center of this grid is referred to as the center point and the valency of this Center point is four.

Step 3. We then consider the coordinate error distribution of a printer and translate it to each of the four Voronoi sites treating these sites as the origin for the translated distributions.

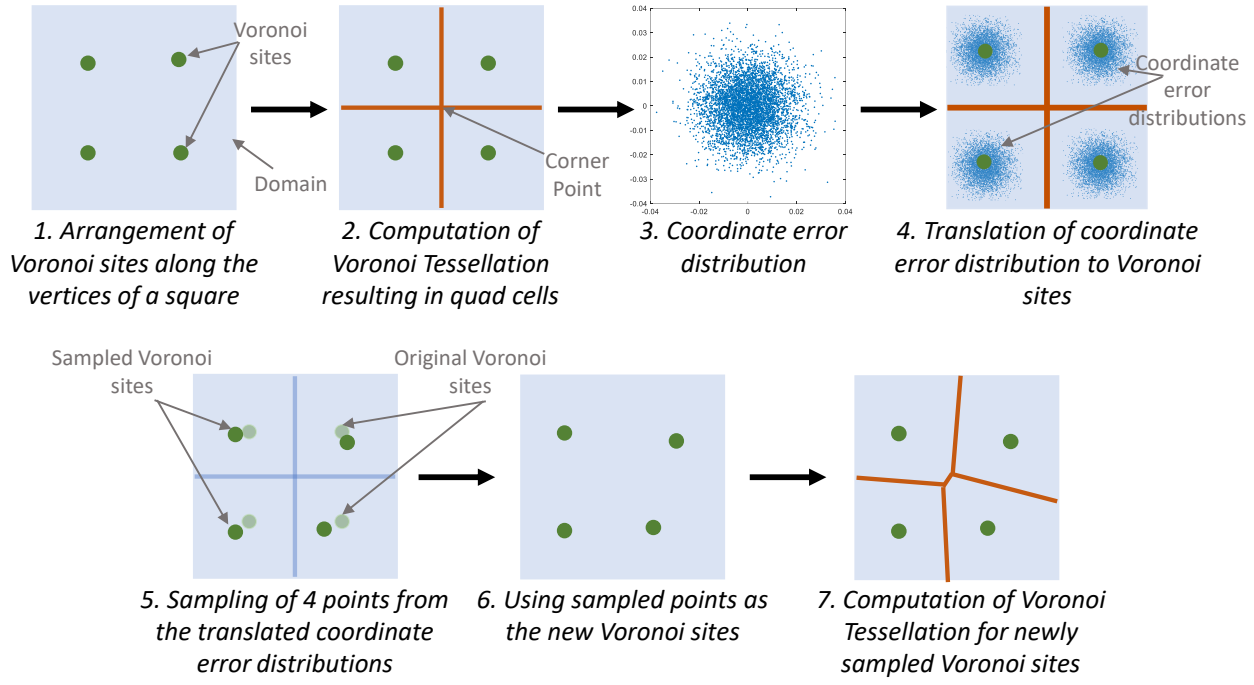

Figure 2.6: Topological Transformation

Thus, we get four translated distributions with same standard deviation but different mean locations.

Step 4. We then sample one point each from all the four translated distributions giving us four new Voronoi sites which are no longer arranged along the vertices of a square.

Step 5. In the final step, we again compute the Voronoi diagram for the newly sampled Voronoi sites. As the new sites are randomly located in the domain, the domain gets decomposed into four unequal Voronoi cells as oppose to a grid of quad cells. Consequently, the four valence center point in the grid splits into a line with three valence endpoints when the Voronoi sites are displaced. This line is known as the Split Edge.

This whole process is called Topological Transformation. Through this process we transform the printer error distribution into a split edge.

It is important to note here that even small changes in the location of the Voronoi sites can be very easily detected and accurately captured in the resulting Voronoi tessellation. This is possible

because of the topology change occurring during the transformation process. In this case, we observe topology change as the center point, a four valence point splits into the split edge. Hence, we utilize the Split Edge as our leading point for further work.

2.7 Evaluation Metric

As the split edge is indicative of the printer error, we utilize it as the basis of our evaluation. Hence, it is important to first parameterize it.

Any straight line in 2D space can be completely defined with any of the following combination of parameters:

1. The length of the line and angle with respect to the horizontal axis along with the location of its midpoint

2. The location of two endpoints of the line

Here, the location of the midpoint and endpoints can be expressed either in cartesian coordinates or in polar coordinates. In polar coordinates, the midpoint can be represented by the length and angle of the line joining the midpoint to the origin. The endpoints can also be represented as the length and angle of the line joining them and the origin. Similarly, we can use different parameters for completely defining the split edge.

2.8 Design of Scheme

2.8.1 Parameterization of the Split Edge

Our first objective is to find the most useful combination of parameters for defining the split edge. We want to select the one which provides maximum and meaningful exaggeration of the differences in coordinate error distribution of two printers after transformation. We want to select parameters that simplifies the process of differentiation between two printers.

As shown in Figure 2.7, we consider two main combinations of parameters. In the first one, the split edge is represented by the length (l_1) and angle (θ_1) of the split edge with respect to the horizontal axis along with the length (l_2) and angle (θ_2) of the line joining the midpoint (m_p) of

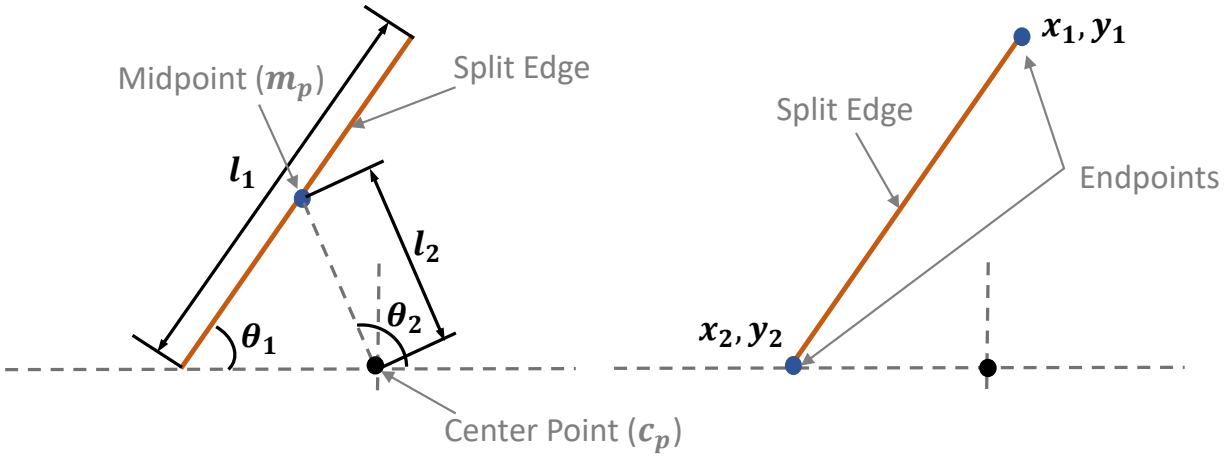

Figure 2.7: Representation of the Split Edge

the split edge and the center point (c_p). And in the second combination, we simply use the x,y coordinates (x_1, y_1, x_2, y_2) of the two endpoints ($e_1p \& e_2p$) of the split edge. We experiment with these two combinations of parameters to select the one that offers the most promising results.

A point to note here is that in both representations, we require four parameters to fully define the split edge i.e. either ($l_1, \theta_1, l_2, \theta_2$) or ($x_1, y_1, x_2, y_2$). This constraint makes our problem, a four variate problem. However, as it is impossible to visualize a four variate problem and as the geometry of the split edge suggests, we convert it into two bi-variate problems. To achieve this, we separate length, angle and midpoint parameters in the first representation method and we separate the two parameters of each endpoint in the second representation method.

2.8.1.1 Generation of Topologically Transformed Error Distribution

As shown in Figure 2.8, for a given coordinate error distribution, we sample multiple sets of four Voronoi sites and compute their Voronoi tessellations. This process generates multiple split edges for the given error distribution of the printer. We present the data generated for multiple split edges in the form of bi-variate probability distributions. In each of the two representation methods of the split edge, we generate two probability distributions which together provide complete data of all the four parameters that are used for defining the split edges.

In the first method, one probability distribution depicts the probability of occurrence of split

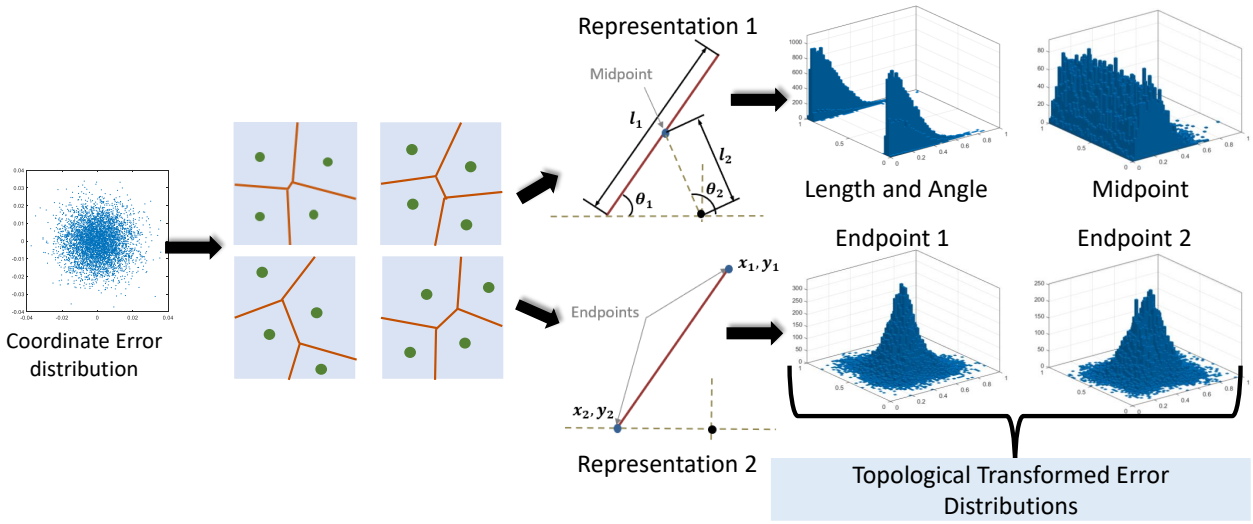

Figure 2.8: Generation of topologically transformed error distributions.

edges with a specific length and angle and the second probability distribution represents the probability of occurrence of split edges with its midpoint at a specific location. These two probability distributions define the coordinate error distribution from which they are generated.

Similarly, the second representation method also gives rise to two probability distributions that defines the original coordinate error distribution. Here, the first probability distribution gives the probability of occurrence of split edge with its first endpoint at a specific location and the second distribution exhibits probability of occurrence of split edge with its second endpoint at a specific location. These bi-variate probability distributions are called as topologically transformed error distributions (Figure 2.8). Thus, each method of split edge representation gives rise to two topologically transformed error distributions which when combined together completely define the given coordinate error distribution of the printer.

2.8.1.2 Comparison of Two Topologically Transformed Error Distributions

In order to be able to characterize printers we have to quantify the differences between coordinate error distributions of two printers. For this, we need to compare the topological error distributions resulting from the topological transformation of coordinate error distributions. One way to do this is to directly compare topologically transformed error distributions resulting from

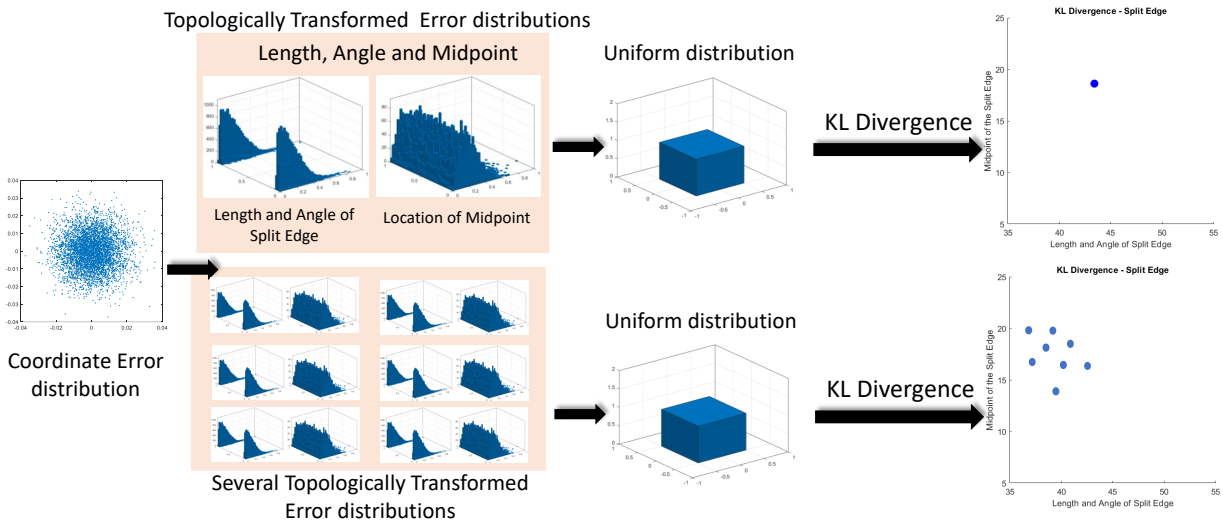

Figure 2.9: Process of representing coordinate error distribution with KL divergence.

two coordinate error distributions.

The other way to do this comparison is to compare all topologically transformed error distributions with a single reference distribution. The advantage of doing this is that we can maintain a common reference point for all distributions irrespective of their mean and standard deviation. Hence, we compare all topologically transformed error distributions with a bi-variate uniform distribution of height $\frac{1}{2\times\sqrt{2}\times 2\pi}$, $\sqrt{2}$ being the maximum length that can be attained by the split edge in a unit square domain and 2π being the maximum angle.

We calculate the difference between the topologically transformed error distributions and the reference uniform distribution in terms of Kullback–Leibler divergence (D_{KL}). Thus, for each representation method, we obtain two KL divergence values resulting from two topologically transformed error distributions. Lower value of KL divergence signifies more similarity between the topologically transformed error distribution and the reference uniform distribution, whereas a higher value signifies less similarity between the two distributions.

In the first representation method, we get a KL divergence value for the probability distribution generated from length and angle of the Split Edge and one for the probability distribution with the midpoint data. In the second representation, we get two KL divergence values for the two

probability distributions generated from the data of the location of the two endpoints. We present both the values emerging from one representation method in a two dimensional scatter plot. Hence, we get two scatter plots for each error distribution, one from length, angle and midpoint and one from the endpoints. In this manner, we have converted the problem from four variate to two variate in both the representation methods.

We sample more points from the same printer error distribution and generate more topologically transformed error distributions. After comparing them with the reference distribution, we get multiple points on the scatter plots. Each point will vary slightly from the other as every point is generated from a different set of randomly sampled points from the same error distribution. Thus, we get a range of KL divergence values for a given coordinate error distributions and any error distribution can be defined using these KL divergence values. Sets of KL divergence values coming from two different coordinate error distributions are directly used for comparing the two distributions and quantifying the difference between them.

2.8.2 Simulated Study

In order to better understand which representation of the split edge will allow meaningful exaggeration of differences in error distribution after transformation, we perform a simulated study. These simulations help us to establish the intuition behind our theory and also provide an understanding of how topological transformation works for different types of input coordinate error distributions. The design, results and analysis of the numerical simulations are presented below.

2.8.2.1 Design

We begin with a unit square centered at the origin. This square forms our domain in 2D space. It consists of four Voronoi sites arranged along the vertices of a square and can be used to decompose the domain into Voronoi cells. Next step would be to translate coordinate error distribution of the printer to each of the four Voronoi sites. For the simulations, we assume printer error distribution to be a bi-variate normal distribution with a specific mean and standard deviation value. At this point, we perform a systematic analysis of the effect of varying mean and standard deviation of the

coordinate error distribution on topological error distributions.

2.8.2.1.1 *Generation of Coordinate Error Distributions* - We generate coordinate error distributions which can be classified into the following two groups:

1. Bi-variate normal distributions with the same mean and varying standard deviation - We generate seven bi-variate normal distributions with their mean at the origin and standard deviation as 0.01, 0.011, 0.2, 0.3, 0.5, 0.6 and 0.08. The variance for these distributions is same in both dimensions and the co-variance is zero. All seven distributions consist of 5000 points.This group of coordinate error distributions helps to study the effect of precision of the printer on the topological transformation process

2. Bi-variate normal distributions with the same standard deviation and varying mean - We generate bi-variate normal distributions with a standard deviation of 0.05 in both the directions and varying means. The co-variance value of these distributions is zero and they consist of 5000 points each. This group talks more about the effect of the bias of the printer.

The location of mean for these distributions are selected in three categories. In category 1, we first select few locations in the first quadrant along the x=y axis at an increasing distance from the origin such as $(0.01, 0.01)$, $(0.011, 0.011)$, $(0.1, 0.1)$, $(0.2, 0.2)$, $(0.21, 0.21)$ and $(0.22, 0.22)$. This would help us to understand the change in behavior of topologically transformed error distributions with increasing distance of mean location from origin. Then in the second category, we select mean locations in the first quadrant along a line with slope of 0.5 like $(0.1, 0.05)$, $(0.2, 0.1)$ and $(0.25, 0.125)$. This would tell us if the nature of the topologically transformed error distributions vary with the change in the slope of the line along which mean location is chosen. Finally, we select some locations in all four quadrants at equal distance from the center and the two axes in the third category. In this category, the means of error distribution are located at $(0.1, 0.1)$, $(-0.1, 0.1)$, $(-0.1, -0.1)$ and $(0.1, -0.1)$. This would help us to understand how the topologically transformed error distributions change with the quadrants in which mean is located but at same distance from the origin.

These error distributions are then translated to each of the four Voronoi sites and 50000 sets of four Voronoi sets are sampled 20 times to get 20 sets of topologically transformed error distributions. This gives us 20 KL divergence values from the length, angle and midpoint of split edges and 20 from the two endpoints. We present these values on two separate scatter plots for comparison between different error distributions.

2.8.2.2 Results After Topological Transformation

1. Bi-variate normal distribution with same mean and varying standard deviation

In this group we compare the results generated for coordinate error distributions with same mean and varying standard deviation after topological transformation. This group gives us an idea of how topological error distributions vary for printers with different precision. We consider seven bi-variate normal distributions with a standard deviation of 0.01, 0.011, 0.02, 0.03, 0.05, 0.06 and 0.08 in both the variables and their mean at $(0, 0)$.

For all coordinate error distributions, we plot their KL divergence values in two scatter plots. The first scatter plot shows KL divergence value for the length and angle of the split edge along the x axis and KL divergence value for the location of midpoint along the y axis. The second scatter plot denotes the relationship between the KL divergence values for the location of the two endpoints for all the error distributions. Each point in these plots is associated with one coordinate error distribution and points of same color belong to the same coordinate error distribution.

In the first plot (Figure 2.10), we observe formation of clusters of different colors along the x axis i.e. along the axis denoting KL divergence value for the length and angle of the edge. The clusters are arranged in the order of decreasing value of standard deviation. The points belonging to coordinate error distribution with standard deviation of 0.01 have the highest KL divergence value for the length and angle of the split edge and the points belonging to the coordinate error distribution with standard deviation of 0.08 have the lowest KL divergence value for the length and angle of the split edge. We do not observe much variation in the KL

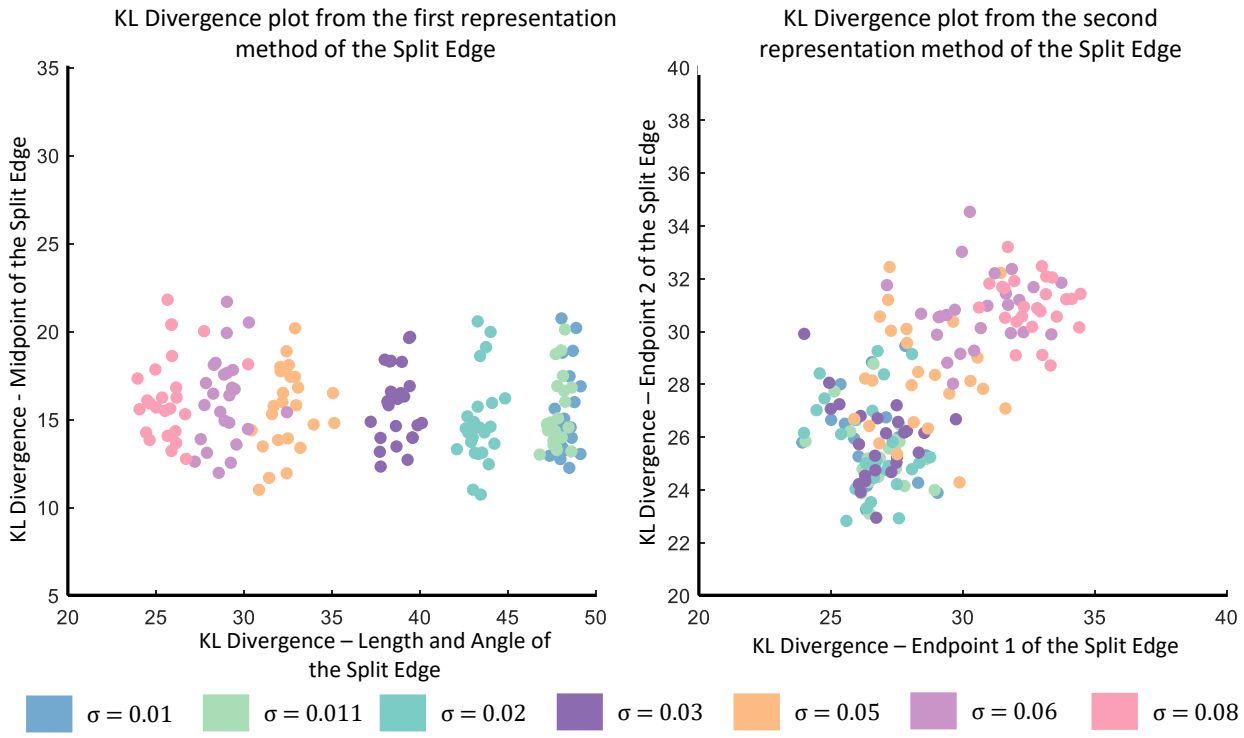

Figure 2.10: KL Divergence Plots generated from length, angle, midpoint and two endpoints for error distributions with same mean and varying standard deviation.

divergence value for the midpoint across all distributions.

Whereas, in the second plot (Figure 2.10) we see clusters roughly forming along the 45 degree line in the increasing order of the standard deviation. However, these clusters cannot be clearly separated according to standard deviations. Thus, for coordinate error distributions with same mean and different standard deviation, maximum exaggeration in the difference between two coordinate error distributions is observed in the first scatter plot that is obtained from the first representation method. Hence, for printers having error distributions with same mean and varying standard deviation, representing split edge in terms of its length, angle and midpoint gives maximum exaggeration between two error distributions.

2. Normal distributions with same standard deviation and varying mean

We study the differences in the error distributions with same standard deviation and different

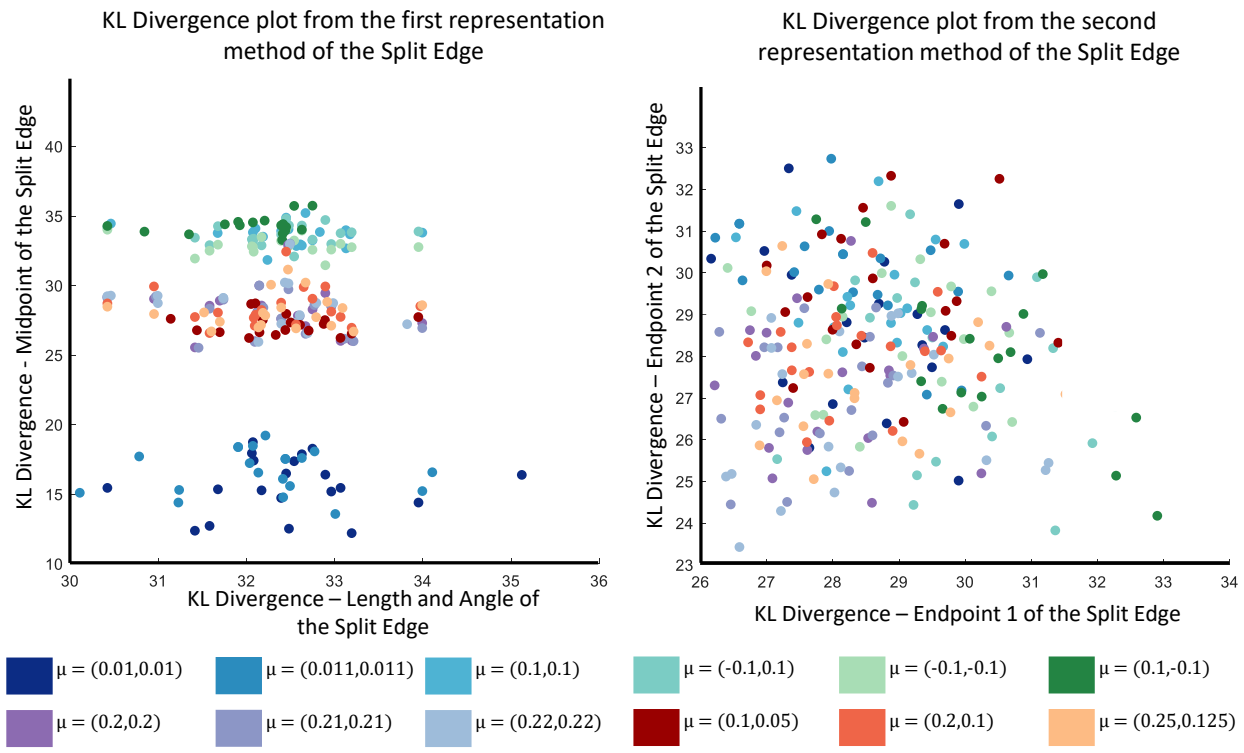

Figure 2.11: KL Divergence Plots generated from length, angle, midpoint and two endpoints for error distributions with varying mean and same standard deviation.

means in this group, thus depicting printers with same precision but different bias.

For this group too, we plot KL divergence values in two 2 dimensional scatter plots (Figure 2.11). In the first plot, we mark KL divergence values for the length and angle of the split edge along the x axis and KL divergence values for the midpoint of the split edge along the y axis. In this plot we observe formation of clusters in some pattern along the y axis. We get three main clusters. The first cluster belongs to error distributions with their means at $(0.01, 0.01)$ and $(0.011, 0.011)$ that is the error distributions that are closest to the origin. Error distributions represented by second cluster have their means at $(0.1, 0.1)$, $(-0.1, 0.1)$, $(-0.1, -0.1)$, $(0.1, -0.1)$. This cluster covers all error distributions in all four quadrants that are at same distance from the origin and the two axes. The last cluster covers error distributions with the means at $(0.2, 0.2)$, $(0.21, 0.21)$, $(0.22, 0.22)$, $(0.1, 0.05)$, $(0.2, 0.1)$

and $(0.25, 0.125)$. This cluster covers error distribution on x=y axis that are farthest from the origin and clusters along the line with slope 0.5. However, we do not notice any variation along the x axis across different distributions.

This shows that topologically transformed error distributions generated from the location data of midpoint are similar for coordinate error distributions with means at equal distance from the origin irrespective of the quadrant in which the mean is located. Thus, their KL divergence value falls in the same cluster. There are no clear differences between topologically transformed error distributions of coordinate error distributions with small difference in their mean location. We also observe that the KL divergence first increases with increasing distance of mean from the origin, then drops and continues to increase later. However, we do not observe any variation with the change in the slope of line along which the mean location is chosen.

We present the second scatter plot, with KL divergence values for the two endpoints of the split edge along the x and y axis. In this plot we do not observe any pattern with increasing distance of mean from the origin or across different quadrants. KL divergence values for all coordinate error distributions contribute to one big cluster. Thus, even for coordinate error distributions with same standard deviation and varying mean, maximum exaggeration in the difference between two coordinate error distributions is observed in the first scatter plot obtained from the first representation method of the split edge. Hence, for characterization of printers having error distributions with same standard deviation but varying means, we use the length, angle and midpoint to represent the split edge.

2.8.2.3 Comparison with Results Before Transformation

For both groups of coordinate error distributions mentioned above, the differences in topologically transformed error distributions obtained from the length, angle and midpoint of the split edge are more dominant than the endpoints of the split edge. This means that we get better characterization of printers when we represent the split edge by its length and angle along with the location

of its midpoint. Further we notice that for coordinate distributions with same mean but varying standard deviation, variation is obtained in the KL divergence values obtained from the length and angle data of the split edge. Therefore, for this group we only concentrate on the topological distributions generated from the length and angle of the split edges. Similarly, for the group of coordinate error distributions with same standard deviation but different means, variation is seen across different distributions when we look at the KL divergence values from the midpoint location data of the split edges. Thus, for this group we use only the results obtained from the length and angle of the line joining the midpoint of split edge and the center point of the domain.

In order to verify if the difference between two coordinate distributions is exaggerated after topological transformation, we compare the results obtained after transformation with the results before transformation. For this, we compare all coordinate error distributions with the reference uniform distribution. This gives us a KL divergence value for each coordinate distribution which we can use to compare the results obtained after transformation.

For coordinate error distributions with their mean at the origin and varying standard deviation, we present KL divergence value for the length and angle of the split edge in a box plot (Figure 2.12). We notice that the median KL divergence value decreases with increasing standard deviation of the error distribution. The median KL divergence value for error distribution with lowest deviation of 0.01 is 48.1490 and the KL divergence value for the highest deviation distribution is 25.8009. In between these two distributions, the KL divergence decreases to 47.7912, 43.3260, 38.6587, 32.4051 and 29.0111 for coordinate error distributions with a standard deviation of 0.011, 0.02, 0.03, 0.05 and 0.06 respectively. Thus, we get a monotonically decreasing behavior of the KL divergence as the standard deviation of coordinate error distribution increases. We also present the results obtained by directly comparing coordinate error distributions to the reference uniform distribution in a separate plot (Figure 2.12). Here we see that we get a KL divergence value of 31.2792 for all the coordinate error distributions making it impossible to differentiate between them.

We perform the same comparison for the group of error distributions with the same deviation but varying mean locations. Here we use the KL divergence obtained from the midpoint location

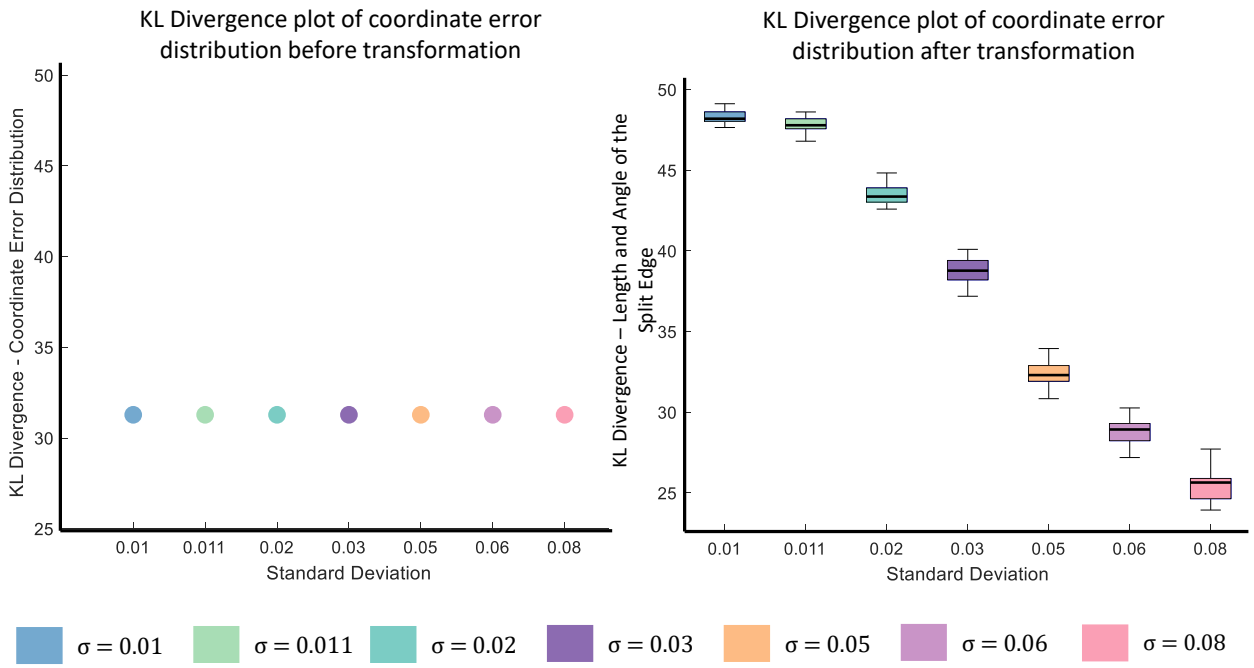

Figure 2.12: KL divergence plotted for coordinate error distributions with same mean and varying standard deviation before applying *SplitCode* and box plot of KL divergence resulting from length and angle of split edges after applying *SplitCode*.

of the split edges and we present them in a box plot (Figure 2.13). From this plot we gain the knowledge of how KL divergence changes with the distance between the mean of error distributions and the origin. The median KL divergence for distributions with their mean at $(0.01, 0.01)$ and $(0.011, 0.011)$ is 15.4593 and 16.9105 respectively. Then as the distance increases such as for error distributions with their mean at $(0.1, 0.1)$, $(-0.1, 0.1)$, $(-0.1, -0.1)$ and $(0.1, -0.1)$, the median KL divergence value also increases to 33.8169, 33.7143, 32.8356 and 34.3296 respectively. After this we observe a drop in KL divergence values as the error distributions move further from the origin. We get a median of 28.3907, 28.3804, 28.7866, 27.2097, 28.1860, 27.9994 for distributions with their mean at $(0.2, 0.2)$, $(0.21, 0.21)$, $(0.22, 0.22)$, $(0.1, 0.05)$, $(0.2, 0.1)$, $(0.25, 0.125)$. This shows that even after the first drop in the KL divergence, we still notice a slight increase with increasing distance of the mean from the origin. Whereas, before topological transformation, we get a KL divergence value of 31.2792 for all coordinate error distributions (Figure 2.13). Thus,

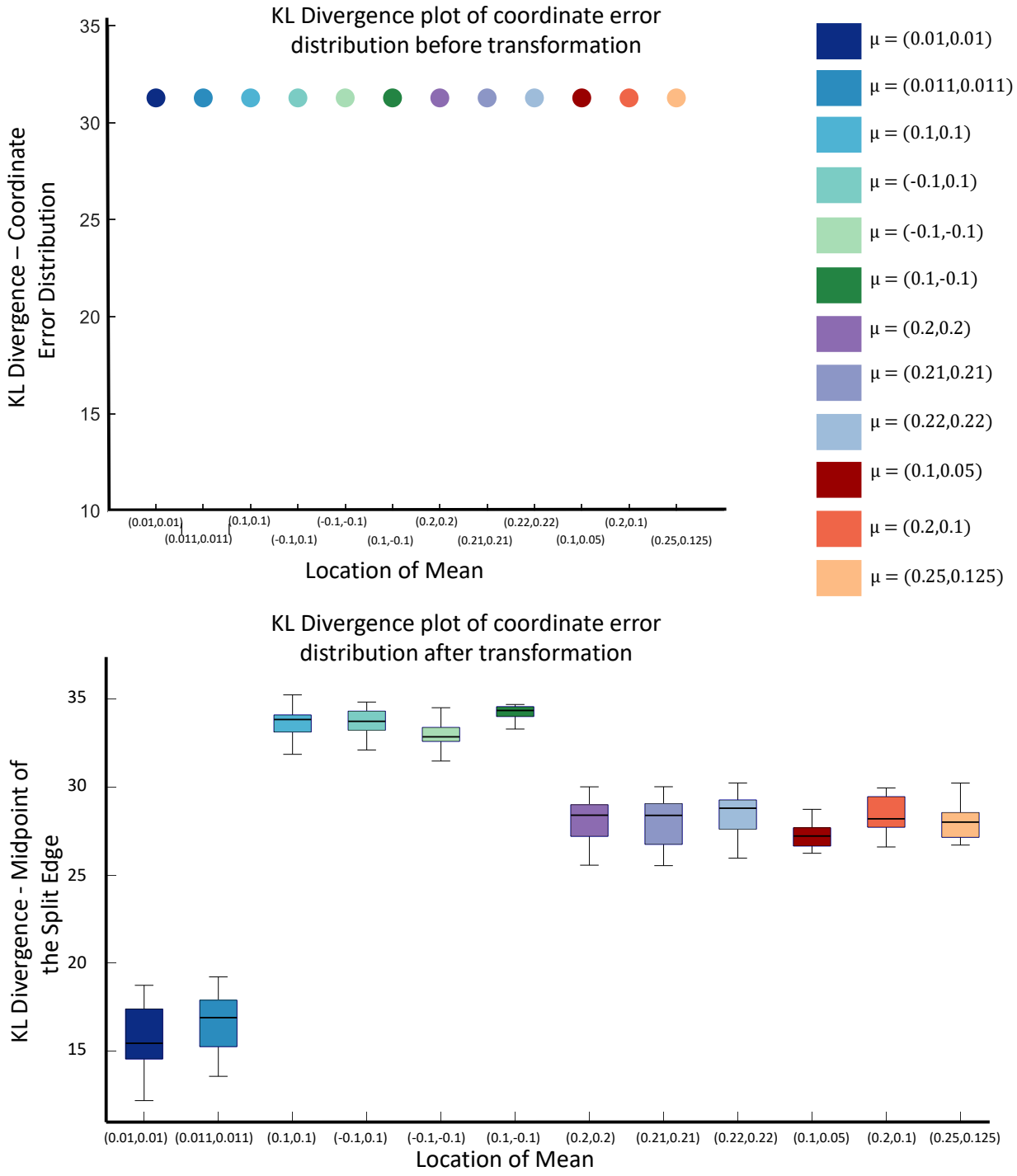

Figure 2.13: KL divergence plotted for coordinate error distributions with varying mean and same standard deviation before applying *SplitCode* and box plot of KL divergence resulting from midpoint location of split edges after applying *SplitCode*.

topological transformation increases the difference between any two coordinate error distributions with varying means and same standard deviation.

2.8.2.4 Conclusion

We observe that by applying *SplitCode* i.e. by topological transformation, we can achieve exaggeration between error distributions of two printers. For distributions with same mean but varying standard deviation, as the standard deviation of the error distribution increases, location of the sampled Voronoi sites move farther from the center point. As a result, we see a clear difference in the length of the Split edge as it increases but not in its location. We see a monotonically decreasing behavior for the KL divergence value obtained from the length and angle of the split edges as the deviation in the error distribution increases.

Whereas, when the location of the mean of error distributions with same standard deviation changes, location of the split edge is affected. No difference is observed in the length of the split edge. Hence, in this case the length and angle of the line joining the midpoint of the Split edge to the center point is more important. Thus for distributions with same mean but varying standard deviation, we can refer to the length and angle data of the split edge and for distributions with same standard deviation and varying means, we can use the midpoint location of the Split Edge. But for both the cases we use the first representation method i.e length, angle and midpoint of the split edge.

From the above results, we can conclude that representation of the split edge in terms of its length (l_1) and angle (θ_1) with respect to the horizontal axis along with the length (θ_2) and angle (l_2) of the line joining its midpoint and the center point provides maximum and meaningful exaggeration of the difference between any two coordinate error distributions. Hence, the length, angle and midpoint of the split edge are most useful parameters for comparing the topological noise of the printers and consequently, for characterization of the printers.

3. Numerical Validation of *SplitCode*

In the previous chapter we introduced a scheme for characterization of 3D printers by comparing the topological noise of printers. We learnt that through topological transformation, we can exaggerate the difference between coordinate error distributions of two printers. The most powerful characterization is obtained when we use the first representation method of the split edge where we represent the split edge with it's length and angle along with the location of it's midpoint. Before applying our scheme on actual 3D printed parts, in this chapter we validate our scheme numerically and also study the effect of different known error distributions on authentication.

3.1 Quality Assessment and Authentication

Authentication starts with a design to be printed on a reference printer and also to print a test print. The design is critical because the coordinate error distributions of the printer and the test print are generated from the error measured in the features printed by the printer. This is followed by imaging of the prints to generate the coordinate error distribution of both the printer and the test print. We then apply topological transformation on the coordinate error distributions to obtain topologically transformed error distributions. By comparing topologically transformed error distributions with a reference bi-variate uniform distribution, we get a reference set of KL divergence values for the printer and another set of KL divergence value for the test print. The next step is to compare these two sets of KL divergence values to find if they belong to the same distribution.

3.1.1 Authentication test

Given a test print and a reference printer, the goal is to be able to identify if the test print is printed on that printer or not. To achieve this we use the KL divergence values generated for both the reference error distribution (r_e) and the test error distribution (t_e). Two sets of KL divergence values act as two distributions. We use single variable Kolmogorov-Smirnov (KS) test to compare the two distributions.

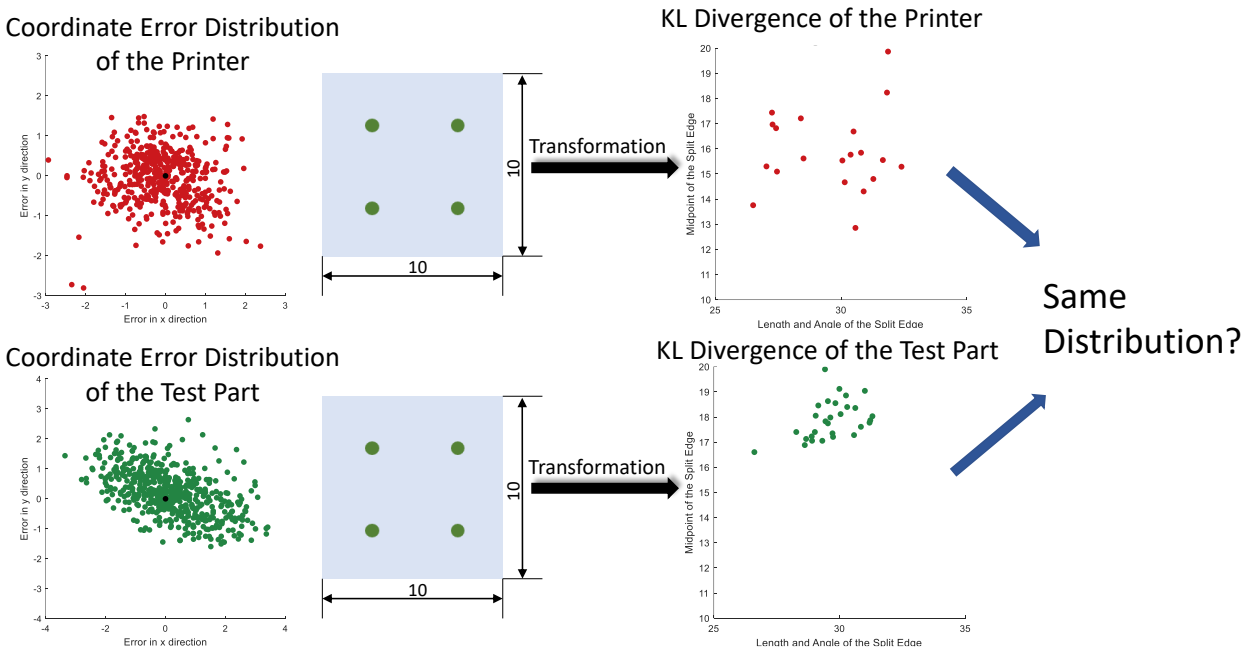

Figure 3.1: Authentication test.

The null hypothesis for this test is that the two distributions, reference KL divergence values and the test Kl divergence values, belong to a common distribution. The alternate hypothesis is that the two distributions come from two different distributions. We get the result of KS test in terms of p value. For example, if p value was 0.3 then there is 30% probability that the two distributions in the test belong to the same distribution. We accept the null hypothesis if p value is greater than or equal to the significance threshold for the reference printer (p_A) and reject it for p value lower than the significance threshold. We will explain significance threshold in detail in the next section.

If the significance threshold for the reference distribution is 0.05, for any p value greater than or equal to 0.05, we accept the null hypothesis and say that the two distributions belong to a common distribution. This means that the test part (t_A) is printed on the reference printer (p_A). However, if the p value is less than 0.05, we accept that the test part was printed on a secondary printer and not on the reference printer.

3.2 Authentication without Topological Transformation

There is one important question that still remains unanswered which is, do we always require topological transformation for authentication. And if we require topological transformation how does it affect authentication. If we had to authenticate 3D printed part without topological transformation, we would have to directly compare the reference coordinate error distribution (r_e) with the test coordinate error distribution (t_e). We could do this through a two variable KS test. Here too the null hypothesis is that the reference coordinate error distribution and the test coordinate error distribution come from a common distribution. And the alternate hypothesis is that the reference coordinate error distribution (r_e) and the test coordinate error distribution (t_e) come from two different distributions. If the p value of the test comes out to be greater than or equal to the significance threshold, we can assume that the two distributions come from the same distribution and there is more probability of the test print (t_A) being printed on the reference printer (p_A). However, if the p value is less than the significance threshold, we can conclude that the test part (t_A) is not printed on the reference printer (p_A).

3.3 Significance Threshold

Significance threshold is the threshold value that helps us to decide if a particular part was printed on a given printer or not. Every printer configuration has a different significance threshold just like how every printer has different error distribution. In order to decide significance threshold for a given printer (p_A), we again use the reference and test error distribution for that printer. To find a significance threshold before transformation, we use the reference coordinate error distribution (r_e) and test coordinate error distribution (t_e) of the printer (p_A). We perform a two variable KS test between these two distributions and find the p value ((p_s)). We know that the two distributions in consideration belong to the same printer.

Now, if we consider a test error distribution for a part that is not printed on the reference printer, after performing the KS test we should be able to identify that this test error distribution and the reference error distribution (r_e) belong to two different distributions. This will be possible if the p

value for this KS test is lower than (p_s). And this is true for any other part that is not printed on the reference printer.

Thus, (p_s) obtained by comparing reference error distribution (r_e) and known test error distribution (t_e) of the same printer is considered as the significance threshold for this printer. Above the significance threshold, we have distributions belonging to the same printer and below the significance we get distributions belonging to different printers. This significance threshold not only varies with the printer, but also depends on the type and number of prints forming the reference error distribution and test error distribution for that printer. Thus, significance threshold for prints printed on the same printer but at different speeds will also be different. To find a significance threshold after transformation, we carry out the same experiment with the reference KL divergence values and test KL divergence values of the given printer (p_A).

3.4 Simulated Validation of *SplitCode*

When two reference coordinate error distributions of two different printers vary significantly in terms of bias or precision, there is a possibility to identify this difference by directly comparing the the two coordinate error distributions. In such a case, performing topological transformation on the two coordinate error distribution might turn out to be redundant. On the other hand, there could be instances where topological transformation is absolutely necessary for authentication. To identify the different cases which will or will not require topological transformation for authentication, we once again take aid of numerical simulations. Here we assume that the error distributions of printers are bi-variate normal distributions with specific mean and standard deviation value.

We perform numerical simulations for four categories of bi-variate normal distributions as follows-

1. Distributions with same mean, zero co-variance but varying standard deviation
2. Distributions with same standard deviation, zero co-variance but varying mean
3. Distributions with same mean, non-zero co-variance but varying standard deviation
4. Distributions with same mean, same standard deviation but varying co-variance

For this, we consider coordinate error distributions two different printers - A & B. For each of the two printers, we generate bi-variate normal distributions consisting of 5000 points each. They form our reference coordinate error distributions for A & B. Then for A & B again, we generate a bi-variate normal distribution with 500 points. These distributions with 500 points form the test coordinate error distributions for A & B. Therefore, reference coordinate error distribution A (ref_A) and test coordinate error distribution A ($test_A$) have the same mean, standard deviation and co-variance. Similarly, reference coordinate error distribution B (ref_B) and test coordinate error distribution B ($test_B$) have the same mean, standard deviation and co-variance. We perform KS tests on (ref_A), (ref_B), ($test_A$) & ($test_B$).

Before topological transformation, we find the significance threshold of reference error distribution A by performing KS test between reference error distribution A (ref_A) and test error distribution A ($test_A$). Similarly, by performing KS test between reference error distribution B (ref_B) and test error distribution B ($test_B$), we get significance threshold of reference error distribution B. We then check test error distribution B ($test_B$) against reference error distribution A (ref_A). Since we are checking the test distribution against reference distribution of A, the resulting p value should be less than the significance threshold of A for us to a get a true negative. Then as we check test error distribution A ($test_A$) against reference error distribution B (ref_B), we will get a true negative if the resulting p value is lower than the significance threshold of B.

After topological transformation we use KL divergence values of all distributions to perform single variable KS test. By comparing KL divergence values of reference error distribution A (ref_A) and test error distribution A ($test_A$), we get a significance threshold for A after topological transformation. Similarly by comparing KL divergence values of reference error distribution B (ref_B) and test error distribution B ($test_B$), we get a significance threshold of B. Later, p values for KS tests between KL divergence values of test error distribution B ($test_B$) and reference error distribution A (ref_A) should be lower than the significance threshold of A and for KS tests between KL divergence values of test error distribution A ($test_A$) and reference error distribution B (ref_B) should be lower than the significance threshold of B. This will give us two true negatives at the

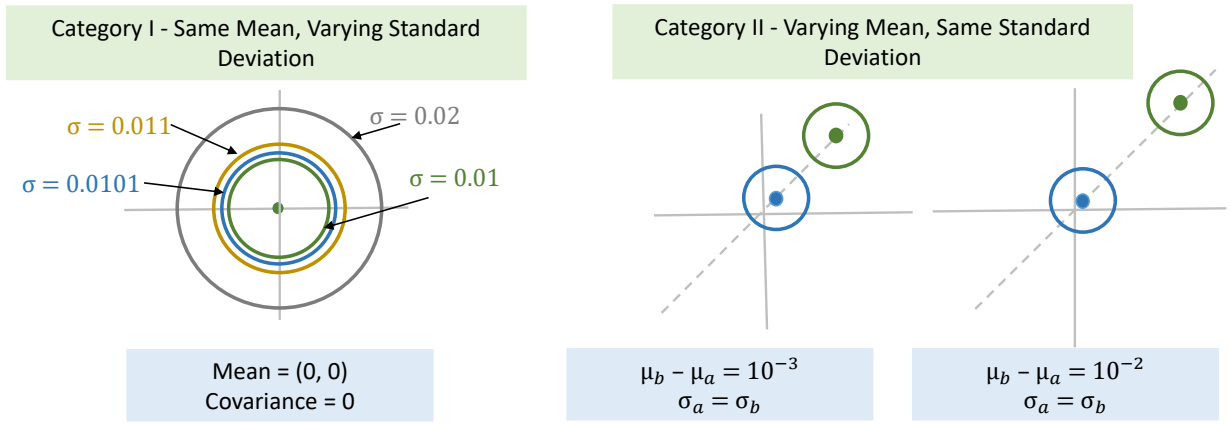

Figure 3.2: Coordinate error distributions with same mean, zero co-variance, varying standard deviation along with coordinate error distributions with varying mean, same standard deviation and zero co-variance.

end.

If towards the end, we have two true negatives, we can assert that we have a case with perfect authentication. However, if we have one false positive or two false positives at the end, we accept that the authentication has failed. Let's look at how the results of numerical simulation look like for different categories of coordinate error distributions.

3.4.1 Distributions with same mean, zero co-variance but varying standard deviation

In this category we study three cases by changing the difference in the standard deviation of the two bi-variate normal distributions (Figure 3.2). The distribution with higher standard deviation signifies error distribution for printers with less precision or prints that are printed on the same printer but higher speed. Prints printed at higher speed will generally have lower precision resulting in more errors and hence, coordinate error distribution with higher standard deviation. In this category we will study if topological transformation is needed or not depending on the difference in the precision of the two distributions that we are comparing.

Significance threshold for A	
Before Transformation	After Transformation
0.5522	0.905

Reference Distribution	Test Distribution	p value - before	p value - after
B	A	0.5982	0.9239

Significance threshold for B	
Before Transformation	After Transformation
0.5522	0.1794

Reference Distribution	Test Distribution	p value - before	p value - after
A	B	0.4633	0.3112

Figure 3.3: Authentication test results for printers having error distributions with same mean, zero co-variance and a difference of 10^{-4} in standard deviation.

3.4.1.1 Case 1. Difference in Standard Deviation = 10^{-4}

Here we have reference error distribution A (ref_A) and test error distribution A ($test_A$) with their mean at the origin $(0, 0)$ and standard deviation of 0.01 in both variables. Co-variance for these two distributions is zero in both dimensions. We also have reference error distribution B (ref_B) and test error distribution B ($test_B$) with their mean at $(0, 0)$, standard deviation of 0.0101 in both variable and zero co-variance. So the difference in the standard deviations of A and B is 10^{-4}.

We get a significance threshold of 0.5522 for reference distribution A and 0.5522 for reference distribution B before topological transformation. When we check reference error distribution A (ref_A) against test error distribution B ($test_B$), we get a p value of 0.4633. This value is lower than the significance threshold of A. Thus we get one true negative result before transformation. We also check test error distribution A ($test_A$) against reference error distribution B (ref_B). We get p value as 0.5982. In this case, the p value is greater than the significance threshold of B which tells us that test error distribution A ($test_A$) and reference error distribution B (ref_B) come from the same distribution. However, as this is not true, we get one false positive before topological transformation.

After transformation, significance thresholds for A and B are 0.905 and 0.1794 respectively. Using these values, we check test distribution B against reference distribution A. We get a p value

of 0.3112 which is lesser than the significance threshold for A. This gives us one true negative. The p value for KS test between test distribution A and reference distribution B is 0.9239 which is a lot higher than the significance threshold of B. This is a false positive result. Thus, for this case both before and after topological transformation we get one true negative and one false positive result. Hence, when the difference in the standard deviation of two distributions or printers is 10^{-4}, authentication fails both before and after transformation.

3.4.1.2 Case 2. Difference in Standard Deviation = 10^{-2}

The reference and test coordinate error distributions A (ref_A & $test_A$) have a standard deviation of 0.01, co-variance = 0, and mean at $(0, 0)$. We have reference and test coordinate error distributions B (ref_B & $test_B$) with mean at $(0, 0)$, co-variance = 0 and standard deviation of 0.02. Thus, the difference between the two standard deviations is 10^{-2}.

For this case, before transformation the significance thresholds for both A and B are 0.5522. p value for KS test between reference error distribution A ref_A and test error distribution B $test_B$ is $9.879\text{x}10^{-25}$. This value is 100% lower than significance threshold of A giving us one true negative result. KS test between reference error distribution B ref_B and test error distribution A $test_A$ gives us a p = $1.781\text{x}10^{-23}$ and another true negative result. This value is also 100% lower than the significance threshold of B. Thus, we get two true negative results before transformation.

After transformation, the significance threshold values for A and B are 0.905 and 0.0893 respectively. Testing KL divergence values of reference A against test B or reference B against Test A gives p = $2.11\text{x}10^{-7}$. This value is lower than significance threshold of A by 99.99 % and 99.99% lower than significance threshold of B. Thus, we have two true negative results after transformation too. For this case, we get two true negatives both before and after transformation. Thus authentication is possible in both the situations. But the decrease in the p values with respect to the significance threshold is more before transformation. Hence, for two printers having error distributions with a difference of 10^{-2} in the standard deviation, authentication is possible both before and after transformation but the accuracy of authentication reduces after topological transformation.

Significance threshold for A	
Before Transformation	After Transformation
0.5522	0.905

Reference Distribution	Test Distribution	p value - before	p value - after
B	A	10^{-25}	10^{-07}

Significance threshold for B	
Before Transformation	After Transformation
0.5522	0.0893

Reference Distribution	Test Distribution	p value - before	p value - after
A	B	10^{-23}	10^{-07}

Figure 3.4: Authentication test results for printers having error distributions with same mean, zero co-variance and a difference of 10^{-2} in standard deviation.

3.4.1.3 Case 3. Difference in Standard Deviation = 10^{-3}

Here, we have reference and test coordinate error distributions A (ref_A & $test_A$) with a standard deviation of 0.01, co-variance = 0, and mean at $(0, 0)$ and reference and test coordinate error distributions B (ref_B & $test_B$) with mean at $(0, 0)$, co-variance = 0 and standard deviation of 0.011. Thus, the difference between the two standard deviations is 10^{-3}.

In this case, the significance thresholds for both A and B are 0.5522 before transformation. KS test between reference error distribution A ref_A and test error distribution B $test_B$ gives p value = 0.0501 which is 90.92% lower than significance threshold of A. KS test between reference error distribution B ref_B and test error distribution A $test_A$ gives us a p = 0.0505. This value is lower than the significance threshold of B by 90.85%. Thus, we get two true negative results before transformation.

After transformation, the significance threshold values for A and B are 0.905 and 0.0626 respectively. Testing KL divergence values of reference A against test B gives p = 0.000023 and testing KL divergence values of reference B against Test A gives p = 0.0199. These values are lower than their corresponding significance threshold values by 99.99% and 68.21%. Thus, we have two true negative results after transformation too.

We get two true negatives both before and after transformation. Thus authentication is possible in both before and after transformation. But the decrease in the p values with respect to their

Significance threshold for A	
Before Transformation	After Transformation
0.5522	0.905

Reference Distribution	Test Distribution	p value - before	p value - after
B	A	0.0501	0.00002

Significance threshold for B	
Before Transformation	After Transformation
0.5522	0.0626

Reference Distribution	Test Distribution	p value - before	p value - after
A	B	0.0505	0.0199

Figure 3.5: Authentication test results for printers having error distributions with same mean, zero co-variance and a difference of 10^{-3} in standard deviation.

significance thresholds is more after transformation than before. Hence, for two printers with error distributions with a difference of 10^{-3} in the standard deviation, authentication is possible both before and after transformation but the accuracy of authentication increases after topological transformation.

3.4.2 Distributions with same standard deviation, zero co-variance but varying mean

In this category we study two cases (Figure 3.2). The difference in the mean locations of two bi-variate normal distributions is different in both the cases. Here, we have printers with different biases and distributions with their mean locations closer to the origin resemble printers with lesser error or parts printed at lower speed and the printers having their error distribution with mean locations farther from the origin showcase higher error.

3.4.2.1 Case 1. Difference in Mean Location = 10^{-3}

Here we have reference error distribution A (ref_A) and test error distribution A ($test_A$) with there means at $(0.01, 0.01)$ and a reference error distribution B (ref_B) and test error distribution B ($test_B$) with their means at $(0.0101, 0.011)$. So the difference in the location of means of A and B is 10^{-3}. All distributions have same standard deviation of 0.05 and a co-variance of zero in both directions.

For this case, we get a significance threshold of 0.5522 for both reference distribution A and reference distribution B before topological transformation. When we check reference error distri-

Significance threshold for A	
Before Transformation	After Transformation
0.5522	0.0463

Reference Distribution	Test Distribution	p value - before	p value - after
B	A	0.5295	0.0463

Significance threshold for B	
Before Transformation	After Transformation
0.5522	0.0034

Reference Distribution	Test Distribution	p value - before	p value - after
A	B	0.328	0.0034

Figure 3.6: Authentication test results for printers having error distributions with same standard deviation, zero co-variance and a difference of 10^{-3} in the mean location

bution A (ref_A) against test error distribution B ($test_B$), we get a p value of 0.5295. This value is lower than the significance threshold of A. We then check test error distribution A ($test_A$) against reference error distribution B (ref_B). We get p value as 0.328. In both the situations, p value is lower than their significance thresholds. This results in two true negatives before transformation.

After transformation, significance thresholds for A and B are 0.0463 and 0.0034 respectively. Taking these values in consideration, we check test distribution B against reference distribution A. We get a p value of 0.0463 which is same as the significance threshold for A. The p value for KS test between test distribution A and reference distribution B is 0.0034 which is also same as the significance threshold of B. Thus, we get two false positives here after topological transformation. From the results, we can infer that when two distributions are separated by a distance of 10^{-3}, authentication is possible before transformation but not after transformation.

3.4.2.2 Case 2. Difference in Mean Location = 10^{-2}

In the second case we increase the distance between the mean locations of two distributions to 10^{-2}. We take distributions with a standard deviation of 0.05 and a co-variance of 0. One reference error distribution A (ref_A) and test error distribution A ($test_A$) have their mean locations at $(0.1, 0.1)$. The means of reference error distribution B (ref_B) and test error distribution B ($test_B$) are located at $(0.11, 0.11)$.

Significance threshold values for both A and B are 0.5522 before transformation and 0.0012

Significance threshold for A	
Before Transformation	After Transformation
0.5522	0.0012

Reference Distribution	Test Distribution	p value - before	p value - after
B	A	0.000523	0.0463

Significance threshold for B	
Before Transformation	After Transformation
0.5522	0.00013

Reference Distribution	Test Distribution	p value - before	p value - after
A	B	10^{-05}	10^{-07}

Figure 3.7: Authentication test results for printers having error distributions with same standard deviation, zero co-variance and a difference of 10^{-2} in the mean location

and 0.00013 respectively after transformation. By comparing reference distribution B with test distribution A, we get p = $1.46\text{x}10^{-5}$ before transformation and p = $5.73\text{x}10^{-7}$ after transformation. Both before and after transformation, the p values are lower than their corresponding threshold values. At this point, we have one true negative both before and after transformation. But when we test reference distribution A against test distribution B, we get p value as 0.000523 before transformation which is lower than the significance threshold of A before transformation. But when we compare the same distributions after transformation, we get a p value higher than the significance threshold. The p value is 0.0463. Thus, in this case too authentication is possible before transformation as we get two true negatives. But after topological transformation, we get one true negative and one false positive making it impossible to authenticate between printers of different biases after transformation.

3.4.3 Distributions with same mean, non-zero co-variance but varying standard deviation

This category is a variation of the first category. Here also we also consider two cases where the differences in the standard deviation of two distributions are different (Figure 3.8). But these distributions have a different bias than the distributions in the first category as these distributions have a non - zero co-variance in both directions. These distributions form an elliptical shape as oppose to circular distributions in the first two categories. Same as the first category, here distributions with lower standard deviation means lesser error. These distributions can be related

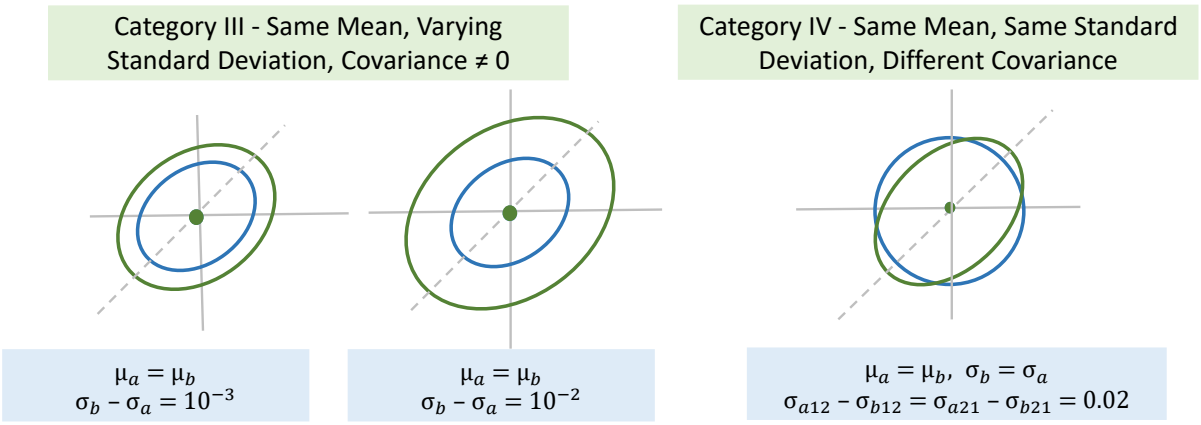

Figure 3.8: Coordinate error distributions with same mean, non-zero co-variance, varying standard deviation along with coordinate error distributions with same mean, same standard deviation and varying co-variances.

to printers with higher precision or to the part in general that are printed with high precision. Whereas, distributions with higher standard deviation resemble to the lower quality prints with more errors.

3.4.3.1 Case 1. Difference in Standard Deviation = 10^{-3}

To simulate this case, we generate reference (ref_A) and test ($test_A$) coordinate error distributions A with a standard deviation of 0.05. We generate another pair of reference (ref_B) and test ($test_B$) coordinate error distributions of B with a standard deviation of 0.051. The difference between the two standard deviation values is 10^{-3} and all distributions have a co-variance of 0.0004 in both direction with their means located at $(0, 0)$.

Before transformation, the significance threshold of A is 0.2975 and significance threshold of B is 0.2742. The p value for KS test between reference error distribution A (ref_A) and test error distribution B ($test_B$) turns out to be 0.2591 which is lower than the significance threshold of A. However, on performing KS test between reference error distribution B (ref_B) and test error distribution A ($test_A$), we get p value = 0.358. This value is higher than the significance threshold of B. Therefore, we get one true negative and one false positive result before transformation.

The significance threshold values of A and B after transformation are 0.0041 and 0.0656 re-

Significance threshold for A	
Before Transformation	After Transformation
0.2975	0.041

Reference Distribution	Test Distribution	p value - before	p value - after
B	A	0.2591	0.041

Significance threshold for B	
Before Transformation	After Transformation
0.2742	0.0656

Reference Distribution	Test Distribution	p value - before	p value - after
A	B	0.358	0.1535

Figure 3.9: Authentication test results for printers having error distributions with same mean, non-zero co-variance and a difference of 10^{-3} in standard deviation

spectively. When we test reference distribution A against test distribution B, we get a p value same as that of the significance threshold of A that is 0.041. This gives a false positive result after transformation. Further, when we test reference distribution B against test distribution A, we get p = 0.1535 which is higher than the significance threshold of B. Thus, we get a total of two false positive results after topological transformation. Hence, authentication fails both before and after transformation when we have two printers having error distributions with same mean, non - zero co-variance and a difference of 10^{-3} between the two standard deviation values.

3.4.3.2 Case 2. Difference in Standard Deviation = 10^{-2}

In this case too we consider distributions with their means located at the origin and have a co-variance of 0.0004 in both direction. The standard deviation of reference error distribution A ref_A and test error distribution A $test_A$ is 0.05 and the standard deviation of reference error distribution B ref_B and test error distribution B $test_B$ is 0.06. Hence, the difference between the standard deviation of A and B is 10^{-2}.

In this case, the significance thresholds for A and B are 0.2975 and 0.1091 respectively before transformation. KS test between reference error distribution A ref_A and test error distribution B $test_B$ gives p value = 0.0516 which is 82.65% lower than significance threshold of A. KS test between reference error distribution B ref_B and test error distribution A $test_A$ gives us a p = 0.0009. This value is lower than the significance threshold of B by 99.17%. Thus, we get two true

Significance threshold for A	
Before Transformation	After Transformation
0.2975	0.041

Reference Distribution	Test Distribution	p value - before	p value - after
B	A	0.0516	0.0001

Significance threshold for B	
Before Transformation	After Transformation
0.1091	0.4333

Reference Distribution	Test Distribution	p value - before	p value - after
A	B	0.0009	0.0006

Figure 3.10: Authentication test results for printers having error distributions with same mean, non-zero co-variance and a difference of 10^{-2} in standard deviation

negative results before transformation.

After transformation, the significance threshold values for A and B are 0.041 and 0.4333 respectively. Testing KL divergence values of reference A against test B gives p = 0.0001 and testing KL divergence values of reference B against Test A gives p = 0.0006. These values are lower than their corresponding significance threshold values by 99.75% and 99.86%. Thus, we have two true negative results after transformation too.

We get two true negatives both before and after transformation. Thus authentication is possible in this case both before and after transformation. But the decrease in the p values with respect to their significance thresholds is more after transformation than before. Hence, for two distributions with same mean, non zero co-variance and a difference of 10^{-2} in the standard deviation, authentication is possible both before and after transformation but the accuracy of authentication increases after topological transformation.

3.4.4 Distributions with same mean, same standard deviation but varying co-variance

Finally, in the last category we compare two distributions with same mean and standard deviation (Figure 3.8), which means the precision is same for the two printers associated with these distributions. But as the co-variances are different, the bias of the printers are different. We consider reference ref_A and test $test_A$ error distribution A which have their means at $(0, 0)$ and standard deviation of 0.051. The co-variances of these distributions is zero. Then we have another pair

Significance threshold for A	
Before Transformation	After Transformation
0.5522	0.0248

Reference Distribution	Test Distribution	p value - before	p value - after
B	A	0.1635	0.0146

Significance threshold for B	
Before Transformation	After Transformation
0.2742	0.0656

Reference Distribution	Test Distribution	p value - before	p value - after
A	B	0.1769	0.0656

Figure 3.11: Authentication test results for printers having error distributions with same mean, same standard deviation but varying co-variance

of reference ref_B and test $test_B$ distributions B that have a standard deviation of 0.051 and co-variance 0.0004 in both the directions. These two distributions also have their means at the origin $(0, 0)$. In this case, we have a circular distribution A and an elliptical distribution B.

Significance thresholds of A and B before transformation are 0.5522 and 0.2742 respectively. After transformation, these values change to 0.0248 and 0.0656 for A and B respectively. On testing reference distribution A and test distribution B, we get p value = 0.1635 before transformation and p value = 0.0146 after transformation. Both these values are lower than their corresponding significance threshold values. Thus, we get one true negative before transformation, as well as after transformation.

When we perform a KS test between reference error distribution B ref_B and test error distribution A $test_A$, we get p = 0.1769. This value is also lower than the significance threshold of B before transformation. Now we have two true negative results before transformation. However, after transformation we get a p value of 0.0656 which is same as the significance threshold of B after topological transformation. We consider this result as a false positive which takes our total to one true negative and one false positive after transformation. From these results, we can see that for distributions with same mean and standard deviation but a difference of 0.0004 in the co-variance, authentication is possible before transformation but not possible after transformation.

3.4.5 Summary of Numerical Validations

From the results presented in the above section, we can conclude that the effect of topological transformation on quality assessment and authentication highly depends on the relative nature of the coordinate error distributions.

Topological transformation is observed to increase the accuracy of authentication when the two distributions in comparison belong to prints printed with different precision but same bias. Prints printed with lower precision can be easily identified when compared to prints printed at a higher precision. Thus, quality assessment becomes the basis of authentication in such cases. This emphasizes on the quality-centric approach of authentication. Whereas, topological transformation may not be effective always while identifying prints that are printed on printers with different bias. In such cases, authentication without topological transformation gives accurate results.

However, the difference in the precision or bias of two prints also plays an important role in authentication both before and after transformation. Depending on this value, we might land up in a situation where authentication both before and after transformation could be possible or may not possible. With these results in mind, for a given pair of reference and test error distribution, we can determine if topological transformation is necessary for authentication.

3.5 Conclusion

We conclude this chapter by highlighting the fact that quality assessment is the basis of our scheme of authentication. This scheme can be used to identify prints that are printed on a secondary printer with lower precision and also to identify prints that are printed on the same printer but at lower quality. However, the scheme cannot be robustly applied for identifying prints that are printed on printers with same precision but different biases. The effect of topological transformation on authentication also depends on the difference between the precision or bias of two printers. Therefore, using the information gathered during simulated experiments, we can apply topological transformation in certain applicable situations to exaggerate the difference between two printers and thus, improve the accuracy of quality assessment and authentication.

4. Experimental Validation of *SplitCode*

So far, our numerical experiments demonstrate that in the worst case scenario (when the distributions are distinguishable in their original form), the topological transformation increases the accuracy of authentication. We specifically observe this in cases where the difference between the distributions is in their variance. This means whenever two printers have same bias but different precision, we can apply *SplitCode* to improve authentication. But the results also showed that when printers have different biases, that is error distributions with different means or different co-variances, *SplitCode* may not necessarily help in authentication. In this chapter, our goal is to investigate *SplitCode* in real-world settings through physical experimentation. These experiments provide an understanding on the nature of coordinate error distributions that we could possibly get for 3D printers and different hole geometries in different cases.

We concentrate mainly on two types of experiments. In the first one, we apply topological transformation to perform authentication between two different printers. The second experiment specifically focuses on the quality assessment aspect of the scheme. In this case, we use topological transformation to identify parts printed on one printer but with different precision. The following sections provide a detailed explanation of experimental validation by describing the experimental setup, design of prints, specifications of printing and imaging, along with the results obtained.

4.1 Case 1 : Authentication of Prints Printed on Different Printers

4.1.1 Problem Description

The problem that we are addressing in this case is purely related to authentication. In this case, a particular design is being printed on an authentic printer. This print is printed at a particular setting and material to maintain a certain quality requested by the customer. Simultaneously, the same design is being printed on a secondary printer by a counterfeiter with probably a lower quality material. The counterfeiter uses one of the many ways to print a cheaper quality print and provides that to the customer. In such a situation, we want the customer to be able to identify the lower

quality part and detect counterfeiting.

Since the print has been printed at a lower quality, it will tend to have more error than the one printed by the authentic printer. These errors can be measured and compared to the coordinate error distribution of the authentic printer. We want see if topological transformation can exaggerate the difference between the coordinate error distributions of the authentic printer and the print that we want to test. Thus, in this problem, We want to understand if this exaggeration helps in detecting a counterfeited print printed on a printer other than the authentic printer.

4.1.2 Design of Parts

For this experiment we designed a square part of dimensions 55x55x1.2mm in SOLIDWORKS 2019. This part contained 25 circular holes of varying dimensions on it. We chose five different diameters for the circular holes- 2mm, 2.5mm, 3.5mm, 4mm, and 5mm (Figure 4.3). The centers of the holes were arranged in 5x5 grid such that in every alternate row starting from the first one, the circular holes were arranged in the increasing order of their diameter from left to right and in the other rows they were arranged in the decreasing order of the diameters from left to right. Such an arrangement of holes is chosen to check if the diameter and the location of hole affects the error in printing that hole. For this design, we compute error at the centers of the printed circular holes with respect to their ideal locations in the CAD image and generate coordinate error distributions.

4.1.3 Design of Experiment

We used two different printers to print the square part with circular holes. Our first printer was a Creality Ender 3 printer. This printer has a printing bed of size 220x220x250mm and a precision of +-0.1mm. The second printer that we used was a Lulzbot Taz 6 printer which has an accuracy of 0.05 to 0.4mm and printing dimension of 280x280x250mm. The design was sliced in software Cura 4.8.0 and the same G Code was used on the two printers. The nozzle and bed temperature of these printers were maintained at 200°C and 50°C respectively. All the prints were printed on the two printers at a speed of 75mm/sec for the infills and 37.5 mm/sec for inner and outer perimeters. We printed 4 prints of the design on each printer at 100% infill in Polylactic acid (PLA) and with

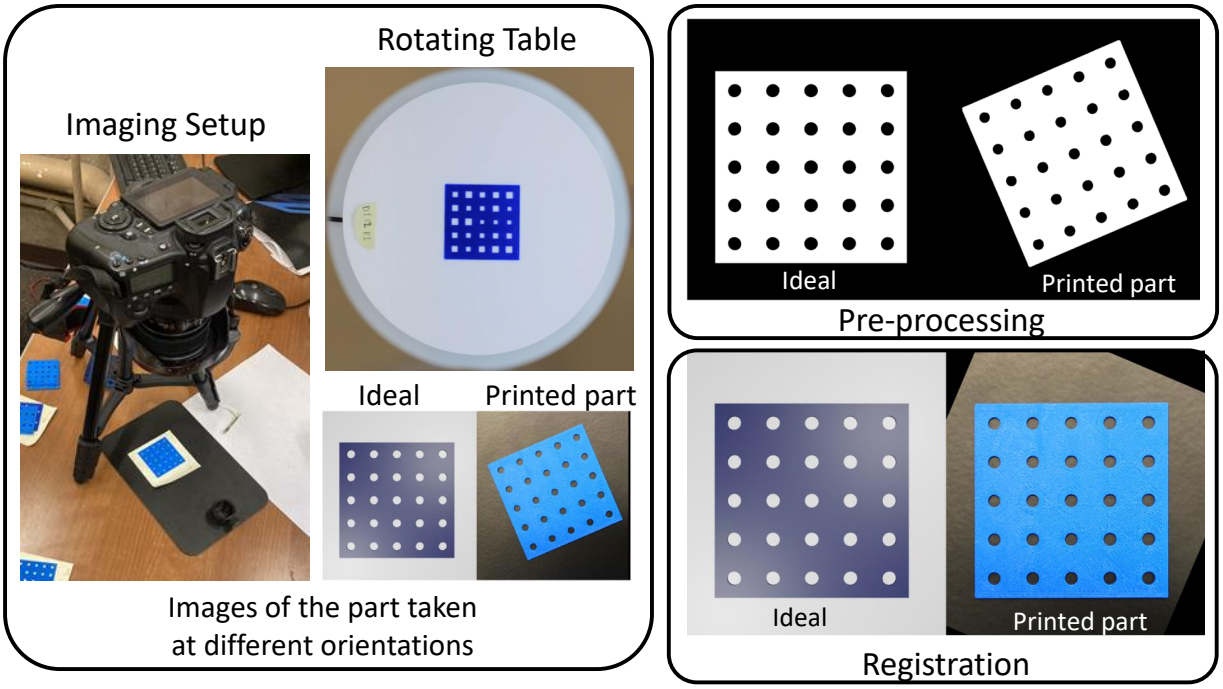

Figure 4.1: Process of capturing images of the prints, processing in MATLAB and registering on the image of the CAD model.

same settings. We used three of these prints printed on each printer to create reference coordinate error distributions of the two printers. The fourth print was used as a test part and to generate test coordinate error distributions.

4.1.4 Measurement of Error and Generation of Coordinate Error Distributions

The process of measuring error in the printed parts is initiated by taking images of the parts (Figure 4.1). For this, we place the print on a rotating table and take multiple images of the print at different orientations ranging from $0°$to $360°$. We used a Canon EOS 60D DSLR with EF 17-40mm F/4 USM lens to capture images of the prints. While doing this, we maintained a neutral lighting condition to minimize the effect of surrounding lights and shadows in error measurement. Taking multiple images of the same print also helped to eliminate some imaging errors and ensuring that authentication was mainly based on the errors caused during printing.

After the images are taken for a given print, the images are processed using MATLAB R2020b.

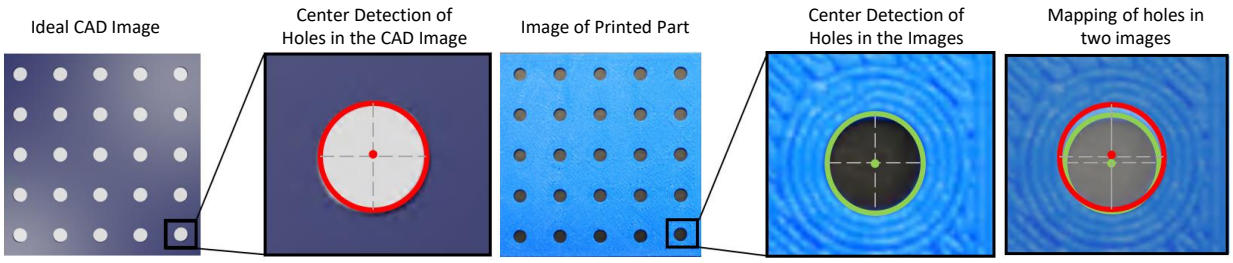

Figure 4.2: Detection of centers of circular holes in ideal CAD image and image of the print and mapping of two images to compute the error in the print.

We first reorient all images and register them on the image of the ideal CAD model. All holes in both the images were detected using circle detection function (imfindcircles) in MATLAB and each hole in the captured image of the print is mapped to its corresponding hole in the image of the CAD model as shown in Figure 4.2. We then find out the centers of the two circles. The shadows in the images play an important role here as it might sometime be mistaken as the boundary of the hole resulting in detection of a smaller hole than actual. We finally measure the length and angle of the line joining the two centers of the two holes in the printed part image and CAD image. Thus, we get error introduced by the printer while printing that particular hole. In the same manner we compute error for all the 25 holes in a part and use that to create the coordinate error distributions of the prints.

The error distributions generated from the reference prints are treated as reference error distributions of the two printers and the coordinate error distributions generated from the test prints are considered as test error distributions for the printers. In this experiment, coordinate error distributions for prints printed on Creality Ender 3 have an elliptical shape (Figure 4.3). We notice that for the first two prints, error distributions are coarser whereas in the other two they are denser at the center. These error distributions are identical to the distributions with mean at the origin and non zero co-variance. Orientation of the error distributions of the four prints roughly tell us about the possibility that they are all printed on the same printer with a specific bias.

On the other hand, coordinate error distributions of prints printed on Lulzbot Taz 6 have circular

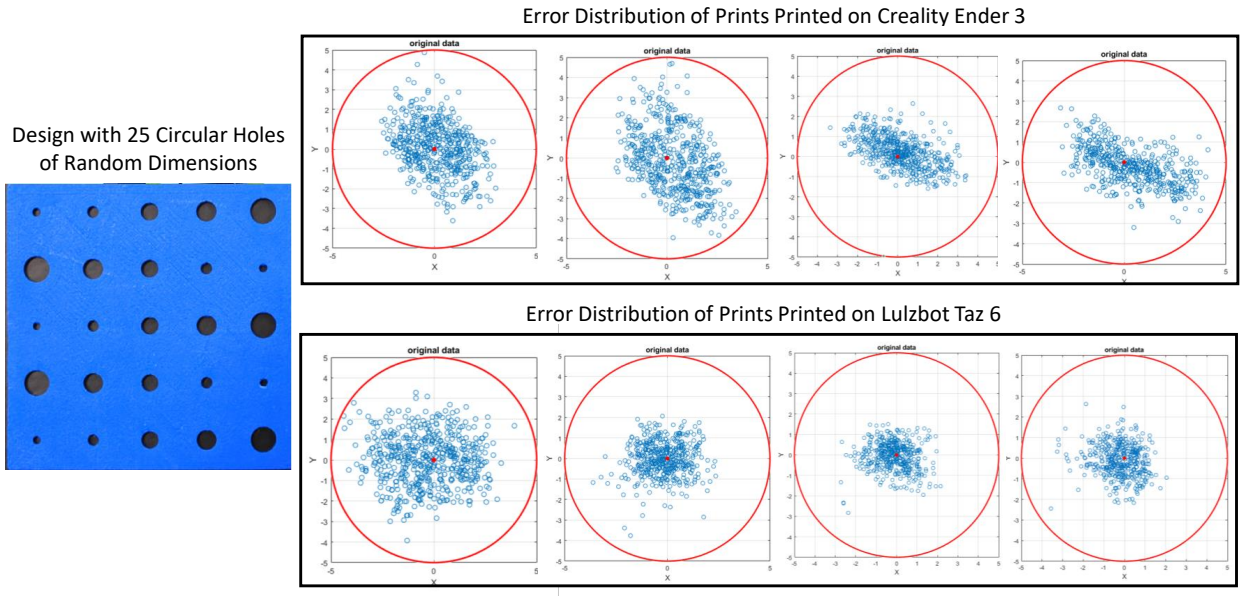

Figure 4.3: Design with 25 circular holes of random dimensions and coordinate error distributions of prints printed on printer Creality Ender 3 and printer Lulzbot Taz 6.

shape (Figure 4.3). Here also, we observe a higher density at the center for 3 prints and a coarser distribution for the other print. These distributions can be related to bi-variate normal distributions with their mean at the origin and co-variance equal to zero. Thus, this experimental case resembles to the simulated case where we had one elliptical and one circular distribution. According to the results of the numerical case, when the difference between the co-variances of two bi-variate normal distributions is 0.0004, authentication is successful before topological transformation but not after. However, in that particular case the difference in co-variances of the two distributions was chosen as low as possible to determine what happens in the extreme situation. In the experimental case the difference in the co-variances of the two distributions is visibly higher than the 0.0004. Hence, it will be interesting to see what happens in this case.

4.1.5 Results of Authentication Before Topological Transformation

Before transformation we first find the significance threshold for the two printers. We will consider the Creality Ender 3 as Printer A and the Lulzbot Taz 6 as printer B. We perform a two variable KS test between reference and test coordinate error distributions of printer A to get

significance threshold for A as 0.0121 and another test between reference and test coordinate error distributions of printer B to get the significance threshold of printer B as 0.0029. With these values as reference, we perform the cross tests.

We get a p value of 10^{-17} for the cross test between reference distribution A and test distribution B. This value is lower than significance threshold of A. This gives us one true negative result. For the other cross test between reference distribution B and test distribution A we get a $p = 10^{-11}$. This value is also lower than the significance threshold of printer B. Hence, we clearly get two true negative results before transformation telling us that test print A is not printed on printer B and test print B is not printed on printer A. From these results, we can tell that authentication for this experimental case is possible without topological transformation.

4.1.6 Results of Authentication After Topological Transformation

We perform similarity test after transformation to see the effect of topological transformation on authentication. Before doing the tests, we plot KL divergence values for the length and angle of split edge v/s the midpoint for all the 8 prints as shown in Figure 4.4. We see a separation between the two printers along the axis with KL divergence values of the length and angle of the split edge. There is no clear difference in the KL divergence values resulting from the midpoint. Hence, we use KL divergence values resulting from the length and angle of the split edges to compare two printers.

From the similarity tests, we get a significance threshold of 0.0429 for printer A and 0.1452 for printer B. We then perform cross tests between the reference and the test error distributions. Cross test between reference distribution A and test distribution B results in p = 10^{-12}. Similarly, cross test between reference distribution B and test distribution A also results in p = 10^{-12}. p values resulting from both the cross tests are lower than their corresponding significance thresholds. Hence, we get two true negative results after transformation too. We can therefore say that, for this experimental case, authentication is possible both before and after topological transformation and there is no particular need of performing topological transformation on the error distributions. Hence, if we have to identify a print printed on a secondary printer with different bias than the

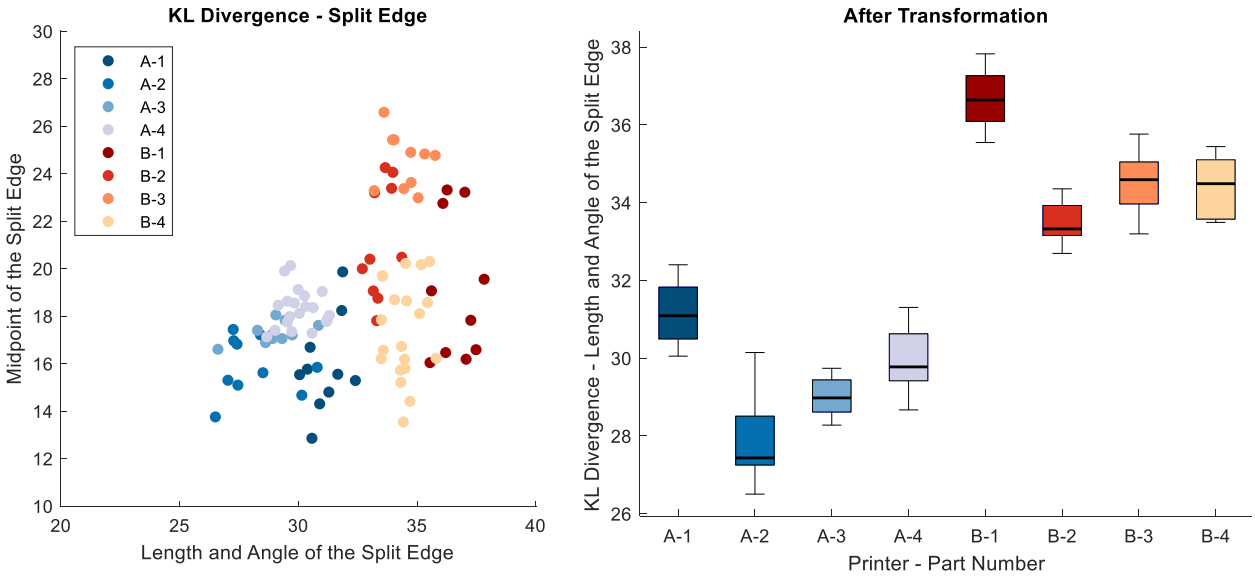

Figure 4.4: Scatter plot for KL divergence of length and angle v/s KL divergence of Midpoint of the Split Edge and box plot of KL divergence of length and angle for all prints printed on Creality Ender 3 and Lulzbot Taz 6.

original printer, we can directly compare coordinate error distributions of the print and the original printer without performing topological transformation on them.

4.2 Case 2 : Quality Assessment of Prints Printed on the Same Printer

In the second experimental problem we want to focus mainly on the quality assessment aspect of the scheme. This test is to catch counterfeiting done on the same printer to print lower quality and cheaper parts. To understand this case, we can assume a design being printed on an authentic printer at a certain speed to maintain the quality of the print. The speed of printing is chosen such as the error in printing is minimized. On the other hand, to reduce the time of printing and eventually to reduce the cost of printing, same design is being printed on the authentic printer but at a higher speed. Another scenario could be that the authentic printer gets attacked by an external source which controls the movement and speed of the printer. Printing at higher speed creates more error in the print thus, reducing the quality of print. As both the prints are printed on the same printer, their coordinate error distributions are likely to have the same mean and bias but different standard deviation. In such a situation, we want the customer to be able to identify

a lower quality print provided by the manufacturer. We conduct topological transformation of the coordinate error distributions to exaggerate the difference between error distributions of prints printed at different speeds.

In order to understand the effect of the geometry of holes on the error distribution, in this case we have conducted one experiments with a design of part with square holes and the other with a design of part with circular holes.

4.2.1 Experiment 1

In our first experiment, we used square holes as our geometric figures to compute error.

4.2.1.1 Design of Parts

To explore this situation, we wanted to select a design where change in error specifically due to change in speed could be measured. We know that when the direction of printing changes, printing speed plays an important role in maintaining the accuracy of printing. Hence, we selected a geometry that has square holes in it and we measured the error at the corners of the squares where the effect of change in speed is more dominantly observed. We designed a square part of dimensions 55x55x1.2mm with 25 square holes on it as shown in Figure 4.8. This design was created in SOLIDWORKS 2019. The centers of these square holes were arranged in a 5x5 grid and the length of their sides were selected randomly from 3mm, 3.5mm, 4mm 4.5mm and 5mm. The size of the square holes was randomly selected on random location to find the effect of size and location of the hole on the error. For this part design, we measured the error at the vertices of the square holes on the printed parts with respect to their ideal locations in the CAD image. The error calculated was then utilized to generate coordinate error distribution of the prints.

4.2.1.2 Design of Experiment

For this experiment, we used a Prusa i3 MK3S which uses its own slicer PrusaSlicer - 2.3.3 for slicing the CAD model. The square part with square holes was sliced in the PrusaSlicer. All parts were printed in Polylactic acid (PLA) by the printer and with an infill percentage of 100 while maintaining nozzle and bed temperature as 210°C and 60°C respectively. We printed two prints

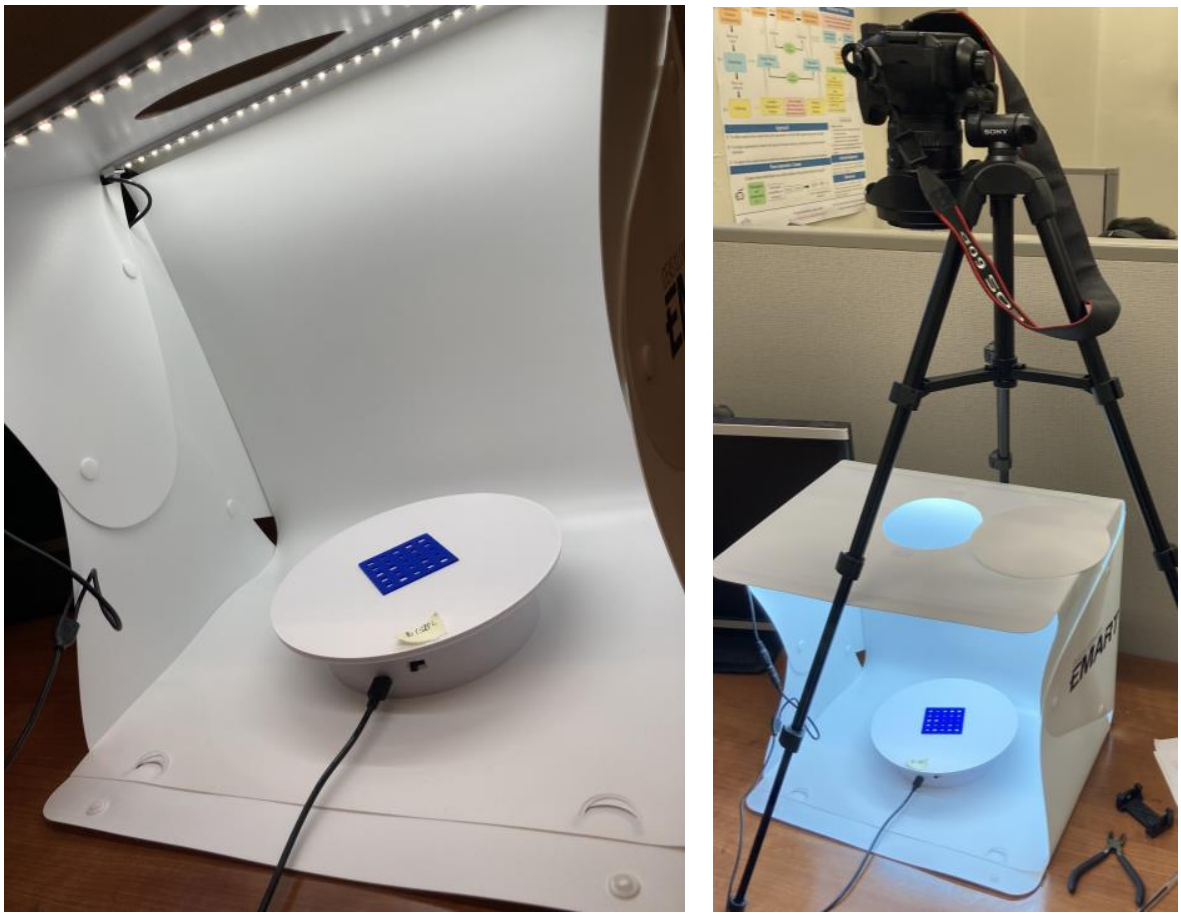

Figure 4.5: Imaging setup comprising of a studio light imaging box and rotating disc used for minimizing error caused due to imaging.

a and b, of the design at a lower speed of 40mm/sec for infill and 30mm/sec for perimeters. One print (a) is used to generate reference error distribution for the prints printed on this printer at this speed. Other print (b) was used a test part at 40mm/sec. Then we printed two more prints c and d, of the design on the same printer at a higher speed of 80mm/sec for infill and 45mm /sec for perimeters. These two prints are treated as the test prints in this experiment. We compute printing error in all four prints and utilize it for authentication.

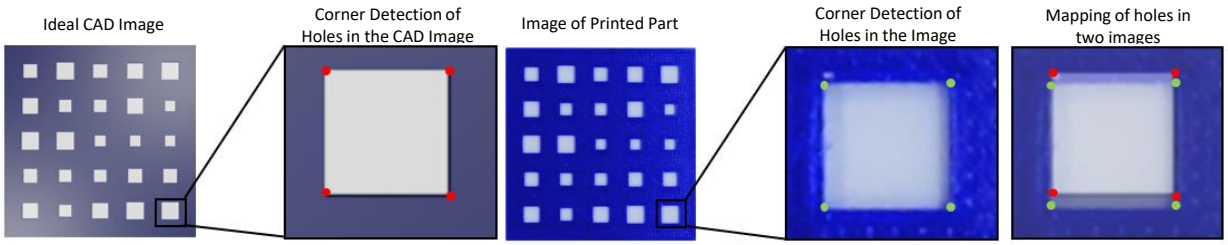

Figure 4.6: Detection of corners of square holes in ideal CAD image and image of the print and mapping of two images to compute the error in the print.

4.2.1.3 Measurement of Error and Generation of Coordinate Error Distributions

The error measurement process for prints with square holes also began with capturing images of the prints. In this experiment we introduced one new object to the imaging setup. As shown in Figure 4.5, we used a white box whose five faces were covered and had a hole on the top for taking images. The rotating table was placed at the center of this box under the hole. This box provided a white background to the images making it easier to process them in MATLAB and it also controlled the light incident on it resulting in minimum imaging error. We took multiple images of a print at different rotations and then reoriented and registered the images on the image of a CAD model (Figure 4.6). After this, we used a corner detection function (detectHarrisFeatures) in MATLAB to detect all the corners in the captured images. At this stage, multiple factors come into picture in the error computation process.

Firstly, because of the noise in the captured images, we do not get straight line edges for the square holes when we process the images in MATLAB. As a result, multiple points are detected in the images by the corner detection function as shown in Figure 4.7. We map all the detected points on the ideal CAD image and find the points that are closest to the actual corners of the square holes on the CAD image. An important point to note here is that, because of the fundamental nature of printing and the thickness of the printing filament, as the printing direction changes by $90°$we do not get a sharp corner. Instead we get fillets. Secondly, when we take images of these prints, shadows increase the probability of detecting a fillet in the location of a corner.

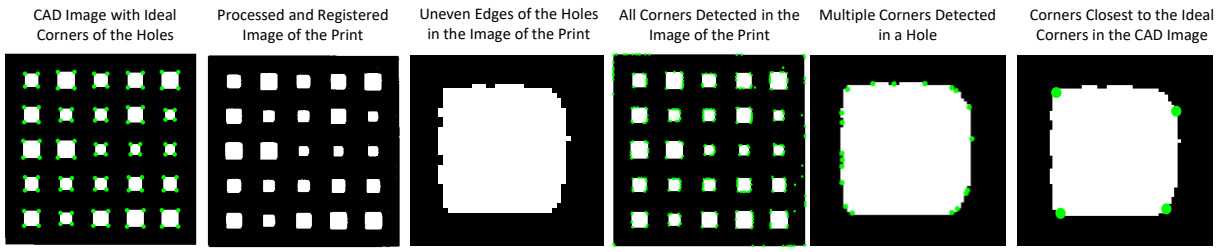

Figure 4.7: This figure shows detection of corners of the square hole in both ideal CAD image and image of the print. Due to uneven edges on the holes in the image of the print, multiple points are detected as corners. We select the points that are closest to the corners detected in CAD image.

Because of the above two reasons, the points detected by the corner detection function often lies on the edges that are incident on the corner. Naturally, the location of the points that are closest to the corners in the CAD image also lies on one of the two incident edges. As a result, when we plot the error to generate coordinate error distribution, we get a diamond-like shape (Figure 4.8). If we compare the error distributions of the prints printed at two speeds, we notice that all distributions have the same bias indicating that they are printed on the same printer or there is a remote possibility that they were printed on printers with same bias but at different speeds. However, we if closely look at the error distributions generated for prints printed at lower speed, we realize that they are denser at the center than the error distributions of prints printed at higher speed. This result follows our intuition of higher error at higher speed. These distributions could be related to the simulated case where we had two distributions with the same mean but varying standard deviation. However, this experiment will also provide us with some understanding on the effect of the hole geometry on error distributions and topological transformation.

4.2.1.4 Results of Quality Assessment Before Topological Transformation

We start by performing a similarity test between the two prints printed at a lower speed that is a and b. These prints are our reference prints as they are printed at a lower speed and have better quality. Similarity test gives us a significance threshold for the prints printed at 30mm/sec on this printer. We get p = 0.0051 for this test. As soon as we get this value, we test the two prints printed at higher speed (c & d) individually with the prints printed at lower speed. When we perform a

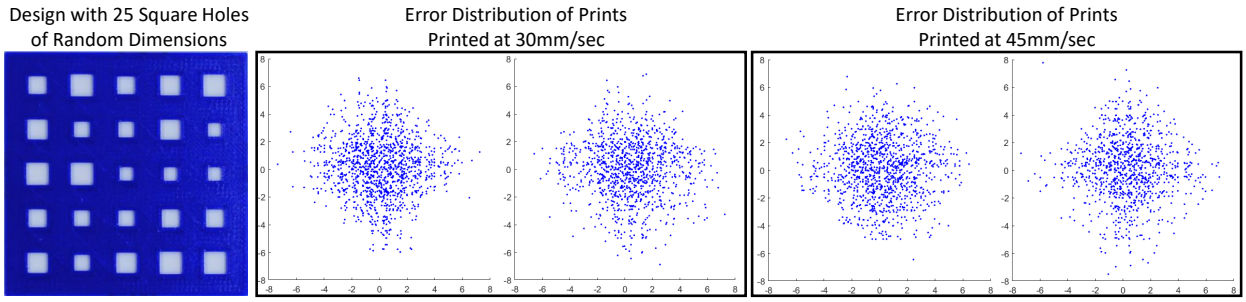

Figure 4.8: Design with 25 square holes of random dimensions and coordinate error distributions of prints printed on printer Prusa i3 MK3S at 30mm/sec and 45mm/sec.

KS test between print c printed at 45mm/sec perimeter speed with prints a& b, we get a p value of 0.4277. This value is higher than the significance threshold. For the test between print d and the reference prints, we get a p value of 0.1671. This test also gives us higher p value than the significance threshold. Thus, we get two false positive results which indicate that prints c and d are printed at the same speed as that of prints a and b. From this we can say that in this case quality assessment is not possible before topological transformation.

4.2.1.5 Results of Quality Assessment After Topological Transformation

In this experiment, as the bias of all distributions is same, we carry out our similarity experiments with the KL divergence values generated from the length and angle of the split edges of the four distributions. We get a significance threshold of 0.9748 for prints printed at lower speed (30mm/sec). The first cross test is performed between print c printed at 45mm/sec and the reference prints. We get p = 0.0946 for this test. Similarly, we perform a cross test between print d and prints printed at lower speed. This test gives a p value of 0.00013. Both the cross tests tell us that the prints c and d are not printed at the same speed as prints a and b. Hence, we get two true negative results and a perfect authentication case. These results prove that if we have to identify parts with square holes that have more error due to being printed at a higher speed, or in simpler terms, has lower quality, topological transformation is necessary.

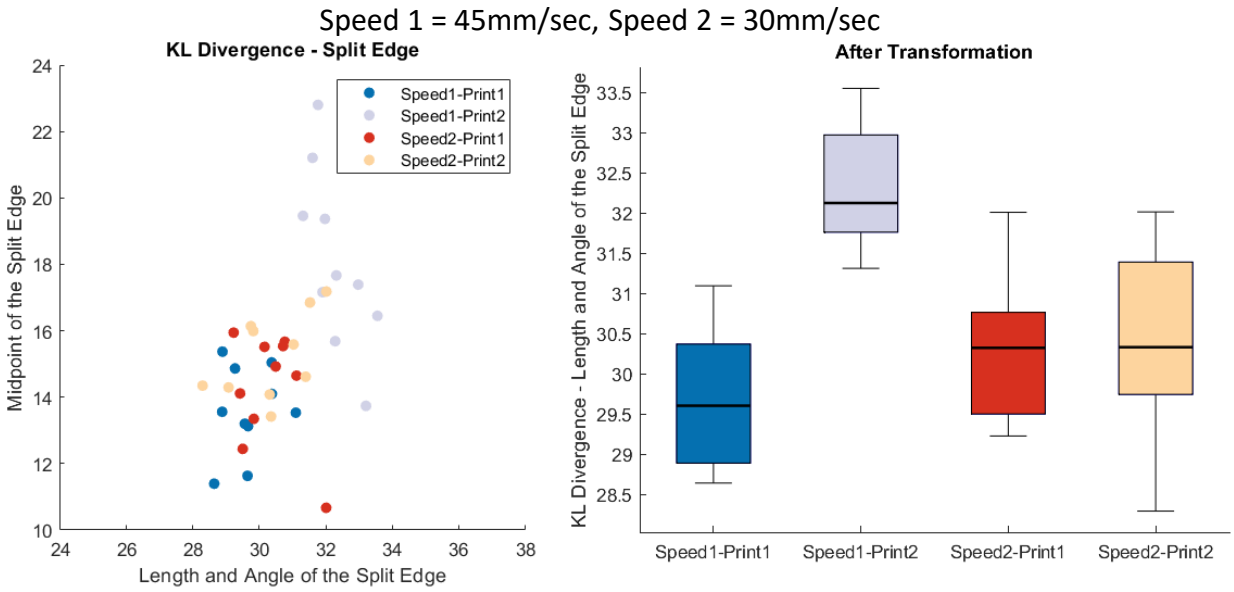

Figure 4.9: Scatter plot for KL divergence of length and angle v/s KL divergence of Midpoint of the Split Edge and box plot of KL divergence of length and angle for all prints printed on Prusa i3 MK3S at 30mm/sec and 45mm/sec.

4.2.2 Experiment 2

We performed one more experiment for the same problem with a design having circular holes on it.

4.2.2.1 Design of Parts

We used the same design for this experiment as the one we used earlier in case 1. The design was a square part of dimensions 55x55x1.2mm which had 25 circular holes of varying dimensions on it (Figure 4.10). Dimensions of these holes range between 2mm and 5mm. The centers of the holes were arranged in 5x5 grid. For this design too, we compute the error at the centers of the printed circular holes.

4.2.2.2 Design of Experiment

We used printer Creality Ender 3 to print the design with circular holes. The design was sliced in software Cura 4.8.0 and the nozzle and bed temperature were maintained at 200°C and 50°C respectively while printing. We printed three prints at a speed of 75mm/sec for the infills and

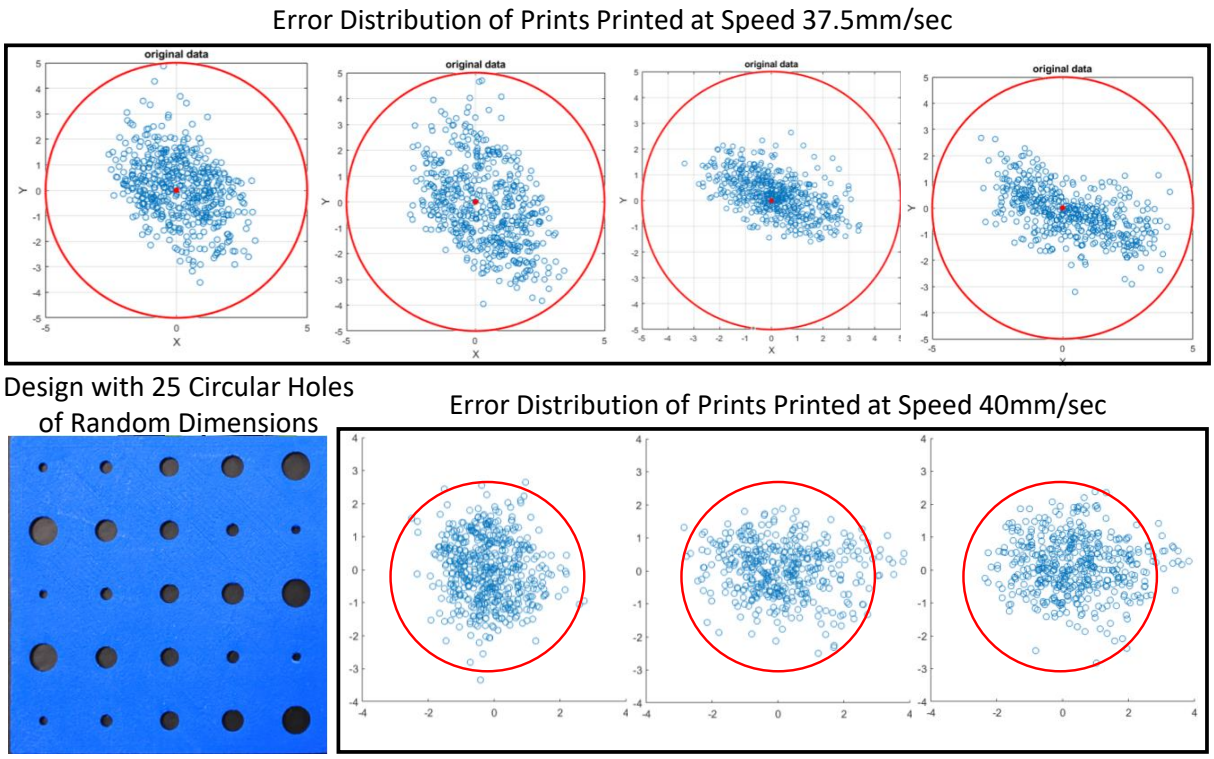

Figure 4.10: Design with 25 circular holes of random dimensions and coordinate error distributions of prints printed on printer Creality Ender 3 at 37.5mm/sec and 40mm/sec.

37.5 mm/sec for inner and outer perimeters. Three more prints were printed at a higher speed of 80mm/sec for infills and 40mm/sec for the perimeters. One print printed at each of the two speeds was considered to be the test print and the other two prints formed the reference sets. All prints were printed with 100% infill in Polylactic acid (PLA). An important note here is that, after printing the parts at lower speed the printer had to undergo a manual calibration which may have changed some printer settings. Keeping this in mind, we generate the reference and test error distributions.

4.2.2.3 Measurement of Error and Generation of Coordinate Error Distribution

The process of measuring error for these prints was same as that of previous experiment done with design with circular holes. Here also, we measured error in a given part by computing error at the centers of the circular holes with respect to their CAD image. We used circle detection function in MATLAB for this purpose. Prints separated to be used as reference contributed in generating

the reference error distributions at the two prints. We get one reference distribution A for speed 37.5mm/sec and another reference distribution B for speed 40mm/sec. Similarly, we generate test distributions A and B for the two speeds. We use these distributions to perform quality assessment tests. (Figure 4.10 shows error distributions of all the prints printed at both the speeds.)

4.2.2.4 Results of Quality Assessment Before Topological Transformation

Before topological transformation, we get two significance threshold values for print printed at higher and lower speeds respectively. Significance threshold for prints printed at 37.5mm/sec is 0.016 and significance threshold for prints printed at 40mm/sec is 1.31x10^{-6} On performing cross test between test distribution B and reference distribution A, we get p = 1.62x10^{-10}. This value is lower than its corresponding significance threshold. When we perform KS test between test distribution A and reference distribution B, we get p = 5.56x10^{-8}. In this case also p value is lower than its corresponding significance threshold. Both the cross tests give us two true negative results as the reference and the test distributions in the cross test are not printed at the same speed. Thus, before transformation we can successfully identify prints with circular holes printed at a different speed.

4.2.2.5 Results of Quality Assessment After Topological Transformation

We use KL divergence values resulting from the length and angle of the split edges to perform similarity tests after topological transformation. Significance threshold values for prints printed at 37.5mm/sec and 40mm/sec are 0.0429 and 0.0012 respectively. First similarity test between reference distribution A and test distribution B gives p = 0.1452 which is higher than the significance threshold of A. This is counted as one false positive result. p value for the second similarity test between reference distribution B and test distribution A is 0.0012. This value is same as its corresponding significance threshold. In total, we get two false positive results after topological transformation and with this the task of quality assessment fails after transformation. So we can say that when we had a problem of identifying a part with circular holes printed on the same printer at a different quality and at a different speed, we were unable to complete the task after applying

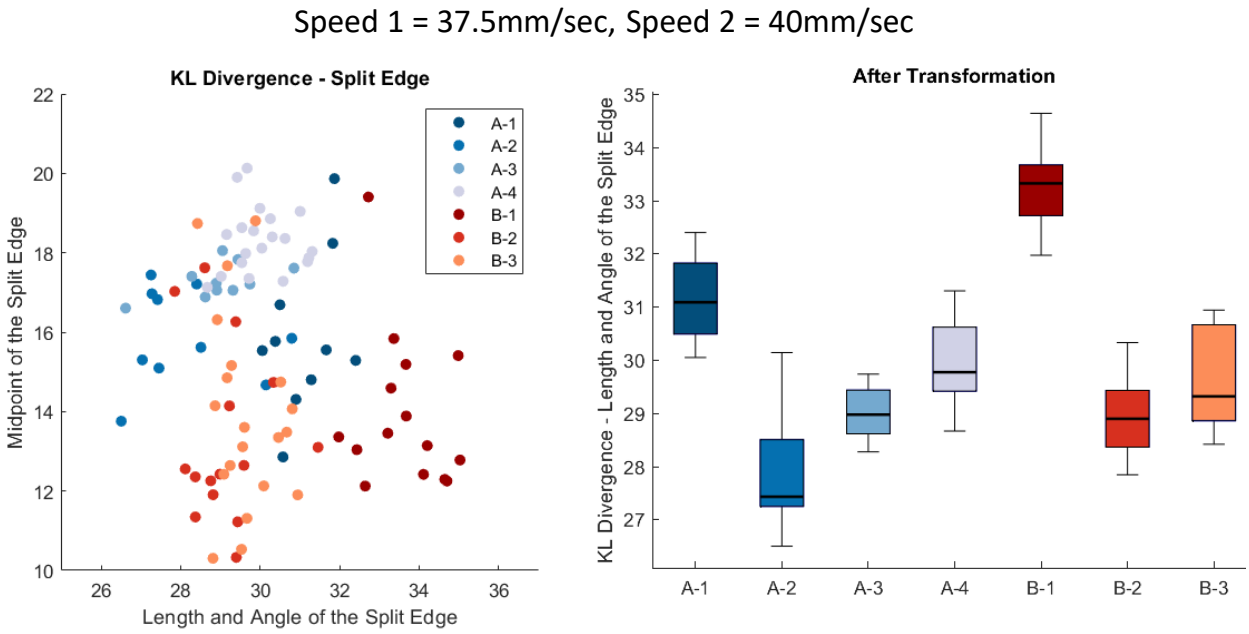

Figure 4.11: Scatter plot for KL divergence of length and angle v/s KL divergence of Midpoint of the Split Edge and box plot of KL divergence of length and angle for all prints printed on Creality Ender 3 at 37.5mm/sec and 40mm/sec.

topological transformation on error distributions. But we could simply perform authentication before transformation.

4.3 Conclusion

The results of the physical experiments provide us with some thoughtful insights. Experiments showed that when the problem is to identify or authenticate a part printed on a secondary printer that has a different bias than the original printer, authentication is possible after applying *SplitCode*. However, even without applying *SplitCode* this authentication could be achieved. When we compare this experiment to the numerical validation case of two distributions with different co-variances, we can say that the difference in the bias of two printers also matter in the accuracy of authentication both before and after topological transformation. On the other hand, when we have to identify a lower quality part printed at a different speed on the same printer, geometry of the holes played an important role. In case of square holes, we required topological transformation for authentication as authentication failed before transformation. However, in case of circular

holes, authentication was only possible before topological transformation and not after. This tells us that the performance of *SplitCode* varies with varying geometries of the holes as geometry has a direct impact on the nature of error distributions. Thus depending on the nature of error distributions, in few cases of authentication between prints printed with different precision but same bias, topological transformation is necessary for quality assessment and authentication. This result once again shows that *SplitCode* is important when the quality of the part changes and also bolsters our quality-centric approach of authentication.

5. Conclusion

This chapter is organized into four sections. In section 5.1, we first summarize the contributions of this research work. We discuss broad implications of the work in section 5.2, followed by highlighting the future directions in section 5.3. Lastly, we end this thesis with some concluding remarks.

5.1 Summary of contributions

This work has four main contributions as follows:

5.1.1 Robust Scheme for Printer Characterization

In this thesis, we first introduce *SplitCode* which is a powerful scheme for characterization of printers through characterizing their bias and precision. We also propose a method of estimating the precision and bias of printers by measuring the errors in the parts printed by the printer and generating coordinate error distributions. *SplitCode* is based on the principle of Voronoi Tessellation and through this scheme we achieve exaggeration of difference between error distributions of two printers. Characterization of printers is important for authenticating parts printed on them. However, differentiating between two printers may not always be feasible by directly comparing the error distributions of two printers. Applying *SplitCode* on the error distributions help us to topologically transform error distributions and exaggerate the error in the printed parts as well as the difference in error distributions of two printers. As a result of this exaggeration, differentiation between two printers becomes easy, enabling us better authentication of additively manufactured parts.

5.1.2 Design of Scheme for Maximum Exaggeration between Error Distributions

We design a scheme for *SplitCode* by selecting the representation of split edge that offer maximum exaggeration of difference between error distributions of two printers. To achieve this we present a simulated study on the effect of varying mean and varying standard deviation of error dis-

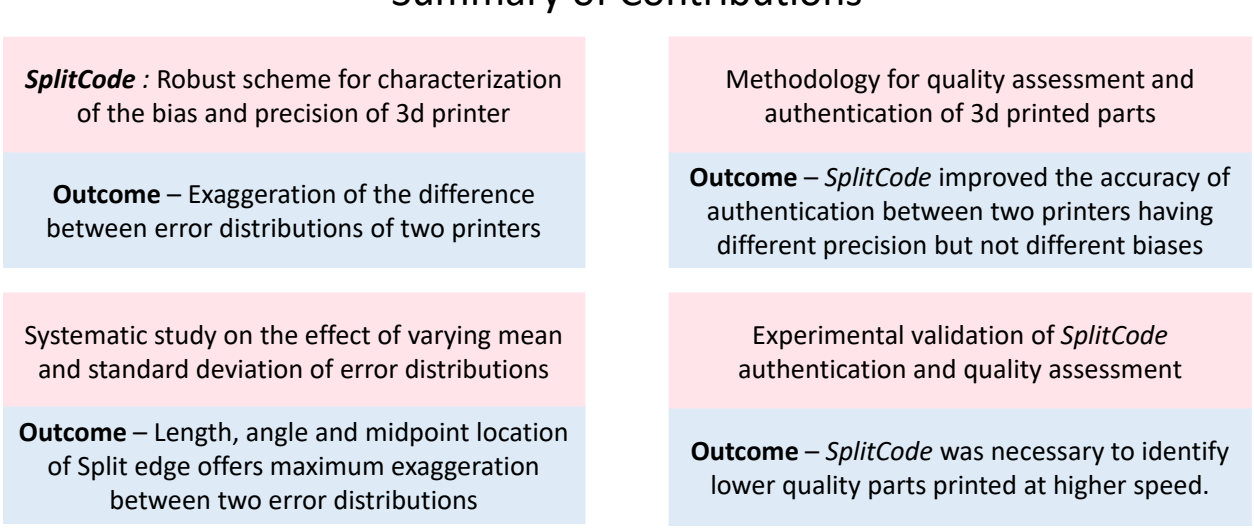

Figure 5.1: Summary of Contributions.

tributions on topological transformation. Through this study, we show that representing the split edge in terms of length, angle and location of its midpoint gives us more meaningful exaggeration between two error distributions. We also find that using the two endpoints of the split edge to define it, we do not get exaggeration between two error distributions thus, giving us a clear indication for selecting length, angle and midpoint to define the split edge. Further, we narrow down our selection of parameters for the two groups of error distributions by concentrating just on the length and angle of the split edge for differentiating between error distributions with same mean and different standard deviation. Similarly, for error distributions with same standard deviation and varying means, we provide evidence that indicate consideration of only midpoint location for differentiation.

5.1.3 Methodology for Quality Assessment and Authentication of 3D Printed Parts

We propose a methodology for conducting authentication and quality assessment tests for additively manufactured parts. We also present a study on the effects of different known distributions on authentication. Through our study we help to build an intuition on application of *SplitCode* for cases where topological transformation improves the accuracy of authentication. We validate our

theory numerically and show that when two printers have error distributions with same mean but different standard deviation, *SplitCode* improves the accuracy of authentication. However, when error distributions of two printers vary in mean location or have different co-variances, *SplitCode* may not necessarily be helpful for authentication. This also means that topological transformation improves accuracy for authenticating parts printed on printers with same bias and different precision but it may not be effective for printers with different biases. In this way, we introduce a quality-centric authentication method.

5.1.4 Guidelines to Apply *SplitCode* in Real Applications

After validating our results numerically, we also present results for quality assessment and authentication of actual 3D printed parts and provide guidelines on application of *SplitCode* in real life applications. Through the experimental results, we once again show that by application of *SplitCode*, we can identify parts printed on an unauthentic printer where the unauthentic printer has different bias than the authentic one. At the same time, when the biases of printers vary from each other by a significant amount we can achieve authentication even before application of *SplitCode*. We also show that when the problem is to identify a lower quality part printed at higher speed on the same printer or printer with same bias, geometry and features used for error estimation affect the accuracy of authentication. According to the results, in some cases topological transformation is absolutely required for authenticating lower quality parts. In other cases, authentication is possible before but not after application of *SplitCode* on error distributions. Thus, from experimental validation we infer that when quality of part changes, topological transformation could be the only way for authentication for certain kinds of error distributions. This emphasizes on the quality-centric aspect of the authentication method.

5.2 Future Implications

This research work has just scratched the surface of a deep concept of quality-centric authentication. It has opened multiple routes for further exploration of this problem. We will discuss some of the implications of this work in this section.

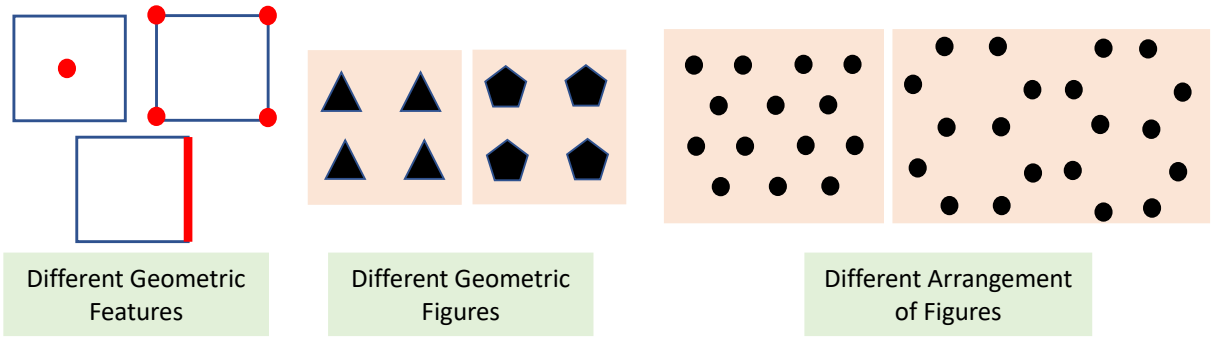

Figure 5.2: Use of different geometric features, figures and arrangement of figures for measuring error in a printed part.

5.2.1 Part Design

In terms of part design, currently we are using centers of circular holes and corners of square holes for estimating error. We have already noticed in our experiments that both the geometry of the hole and the features used for error measurement affect the nature of error distributions and eventually, authentication. In future, an interesting problem is to study the effect of different geometric figures in more detail by selecting figures like triangles, pentagons or hexagons as shown in in Figure 5.2. Experimenting with different features such as centroid, edges or midpoints of edges (Figure 5.2) will give us an understanding on how the estimation of error is affected by the features at which it is calculated. It is also possible to arrange geometric figures in various ways such as in a triangular or hexagonal grid as shown in Figure 5.2. Different arrangement of features for the same part will give different error distributions thus, giving us a more accurate representation of the precision and bias of printers.

5.2.2 *SplitCode* Algorithm

There is great scope of exploration within the algorithm of *SplitCode*. Our algorithm is based on a simple principle of topology change in uniform quad grid structures. Changing this quad grid to other nonuniform Voronoi grid structure (Figure 5.3) will generate different topologically transformed error distributions and provide different amount of exaggeration between two error distributions. In order to increase the sensitivity of topological transformation, arranging Voronoi

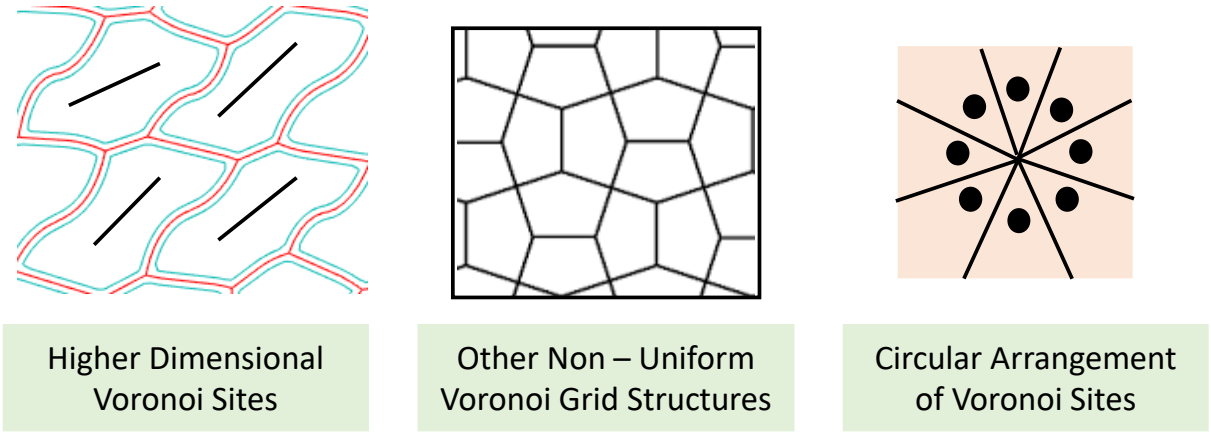

Figure 5.3: Use of higher dimensional Voronoi sites, non-uniform Voronoi grid structures and circular arrangement of Voronoi sites to study the effect on topologically transformed error distributions.

sites in a circle as shown in Figure 5.3 is worth trying. Our method assumes that imprecise nozzle movement is the only cause of error in printed parts. But in reality, even this error could be affected by factors like temperature of the surroundings, temperature of the printer bed and filament quality. In order to properly measure error only due to inexact movement of the printer, we could use higher dimensional Voronoi sites like straight lines or curves (Figure 5.3). These variations in the *Split-Code* algorithm will provide an understanding on which factors affect topological transformation in a positive sense to achieve meaningful exaggeration between two error distributions.

5.2.3 Statistical Variations

Once exaggeration between two error distributions is achieved, the tests used for authentication also affect the performance of authentication. In our work, we use statistical tests that allow use of only two features of the split edge. Instead of considering probability of one split edge to check if the reference and test error distributions belong to the same distribution, using joint probability of a grid of split edges (Figure 5.4) can prove to be a more descriptive representation of an error distribution and hence, improve the accuracy of authentication. Use of multiple split edges and multiple features can be made possible by replacing statistical tests with machine learning algorithms. Another way to get more reliable authentication is to consider location dependent error for

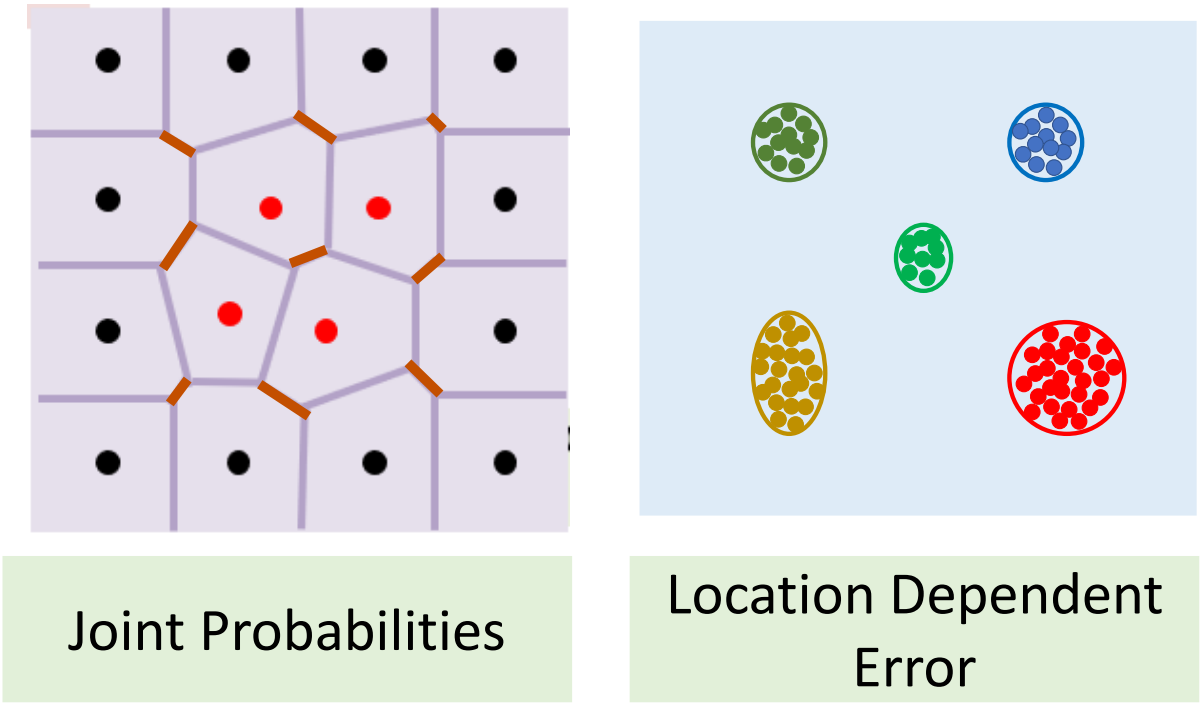

Figure 5.4: Use of joint probability of a grid of split edges or consideration of location dependant error to improve the accuracy of authentication.

a given printed part as shown in Figure 5.4. Because of the hardware imperfections, printer error can vary from one location to the other on the printer bed. Experimenting with location dependent error will offer a way to differentiate between printers that have similar overall error distribution but different error distributions when compared location wise.

5.2.4 Processing Methodologies

Since the process of error measurement in printed parts start with capturing images of the part and processing them, these processes greatly influence the measured error. As seen in our experiments, image processing and feature detection methods can even change the shape of the error distribution. Hence, it is important to correctly detect the features at which error is estimated. In future, use of better post processing methods for RGB images will facilitate accurate detection of features. While taking images, surrounding lights and shadows tend to sway the measurement of

error. Implementing different imaging methods like 3D scans or micro scan can help in eliminating these issues. Finally, utilizing non imaging techniques like acoustic, vibrations or optics for detecting features and errors is also another way to ensure that the error measured is solely caused due to printing.

5.3 Future Works

In this work, we provided a detailed study on the effects of varying mean and standard deviation of error distributions of printers on topological transformation, that is the effect of precision and bias of a printer on error exaggeration. However, at this time we concentrate only on the error that is inherent to the printer. In future, using the results of our study, it is possible to introduce controlled errors in the part while it is being printed. In other words, encoding bias and lack of precision in specific parts while printing will allow us to encode certain information in the parts. This encoded information can then be used for authentication. One simple way to achieve this could be by applying vibration to the printer nozzle.

Our research deals with specific type of counterfeiting resulting due to theft of technical data at the manufacturing level. This method is still limited to authenticating parts printed on different printers and parts printed at different speeds on the same printer. We could extend our work to be more inclusive of other counterfeiting attacks happening at the manufacturing level. Eventually, the goal is to be able to identify the source printer of a given 3D printed part. Simultaneously, we could branch out our study from just flat surfaces to parts with curved surfaces. The main challenge here is to get accurate estimation of the error through imaging. A way to address this challenge would be to resort to advanced scanning techniques or non imaging feature detection.

5.4 Concluding Statement

AM industry is a continuously growing industry and because of its advantages over conventional machining, it has strengthened its roots in all major industries. With the increase in number of applications, this industry has also suffered great losses from attacks like counterfeiting. This has created the need for authentication in AM. Existing authentication techniques involve complex

designing or use of advanced technology, limiting their use in everyday applications. Our research provides a method for authentication and quality assessment of 3D printed parts and addresses some of the existing challenges.

Based on the principle of Voronoi Tessellation, we provide a technique to exaggerate differences between error distributions of two printers. Thus, our method enables characterization of printers based on characterization of their bias and precision and thereby enabling authentication of parts printed on them. Currently, effective in improving authentication in certain cases of identifying lower quality parts, this technique has great potential of increasing the accuracy while authenticating parts printed on different printers and identifying the source printer of a printed part. This work has the capability to create a foundation for encoding information in 3D printed parts by encoding bias and lack of precision while printing. To this end, we believe that this work is just the beginning of exploration of an extremely rich concept of quality-centric authentication.

REFERENCES

[1] T. Campbell, C. Williams, O. Ivanova, and B. Garrett, "Could 3d printing change the world," *Technologies, Potential, and Implications of Additive Manufacturing, Atlantic Council, Washington, DC*, vol. 3, 2011.

[2] M. Attaran, "The rise of 3-d printing: The advantages of additive manufacturing over traditional manufacturing," *Business Horizons*, vol. 60, no. 5, pp. 677–688, 2017.

[3] D. Thomas *et al.*, "Economics of the us additive manufacturing industry," *NIST Special Publication*, vol. 1163, 2013.

[4] D. S. Thomas, S. W. Gilbert, *et al.*, "Costs and cost effectiveness of additive manufacturing," *NIST special publication*, vol. 1176, p. 12, 2014.

[5] B. Hao and G. Lin, "3d printing technology and its application in industrial manufacturing," in *IOP Conference Series: Materials Science and Engineering*, vol. 782, p. 022065, IOP Publishing, 2020.

[6] J. Foust, "Spacex unveils its "21st century spaceship,"," *NewSpace Journal*, 2014.

[7] T. Saraçyakupoğlu, "The qualification of the additively manufactured parts in the aviation industry," 2019.

[8] https://media.gm.com/media/us/en/gm/home.detail.html/content/Pages/news/us/en/2020/dec/1214 additive.html, "General motors increases agility and speed by opening all-new additive industrialization center dedicated to 3d printing," 2020.

[9] C. Li, D. Pisignano, Y. Zhao, and J. Xue, "Advances in medical applications of additive manufacturing," *Engineering*, 2020.

[10] I. Gibson, D. W. Rosen, and B. Stucker, "Medical applications for additive manufacture," in *Additive Manufacturing Technologies*, pp. 400–414, Springer, 2010.

[11] C. Culmone, G. Smit, and P. Breedveld, "Additive manufacturing of medical instruments: A state-of-the-art review," *Additive Manufacturing*, vol. 27, pp. 461–473, 2019.

[12] D. Cohen, M. Sargeant, and K. Somers, "3-d printing takes shape," *McKinsey Quarterly*, vol. 1, pp. 1–6, 2014.

[13] https://www.metal-am.com/3d-hubs-publishes-its-addititive-manufacturing-trend-report 2021/, "3d hubs publishes its additive manufacturing trend report," 2021.

[14] B. Karagöl, "3d printing: What does it offer and for whom," 2015.

[15] F. E. G. de Almeida, "3d printing and new security threats," *Revista Do Instituto Brasileiro De Segurança Pública (RIBSP)-ISSN 2595-2153*, vol. 3, no. 7, pp. 197–210, 2020.

[16] M. Yampolskiy, L. Schutzle, U. Vaidya, and A. Yasinsac, "Security challenges of additive manufacturing with metals and alloys," in *International Conference on Critical Infrastructure Protection*, pp. 169–183, Springer, 2015.

[17] K. V. Wong and A. Hernandez, "A review of additive manufacturing," *International scholarly research notices*, vol. 2012, 2012.

[18] T. D. Ngo, A. Kashani, G. Imbalzano, K. T. Nguyen, and D. Hui, "Additive manufacturing (3d printing): A review of materials, methods, applications and challenges," *Composites Part B: Engineering*, vol. 143, pp. 172–196, 2018.

[19] S. Kuntanapreeda and D. Hess, "Opening access to space by maximizing utilization of 3d printing in launch vehicle design and production," *Applied Science and Engineering Progress*, vol. 14, no. 2, pp. 143–145, 2021.

[20] https://www.space.com/26899-spacex-3d-printing-rocket engines.html, "Spacex taking 3d printing to the final frontier," 2014.

[21] M. Yampolskiy, A. Skjellum, M. Kretzschmar, R. A. Overfelt, K. R. Sloan, and A. Yasinsac, "Using 3d printers as weapons," *International Journal of Critical Infrastructure Protection*, vol. 14, pp. 58–71, 2016.

[22] https://www.additivemanufacturing.media/articles/satellite-to-use-additive-manufactured-components-directly-exposed-to space, "Satellite to use additive-manufactured components directly exposed to space," 2014.

[23] https://www.hubs.com/knowledge-base/automotive-3d-printing applications/, "Automotive 3d printing applications."

[24] https://amfg.ai/2019/05/28/7-exciting-examples-of-3d-printing-in-the-automotive industry/, "10 exciting examples of 3d printing in the automotive industry in 2021," 2019.

[25] https://formlabs.com/blog/3d-printed-car-how-3d-printing-is-changing-the-automotive industry/, "Road to the 3d printed car: 5 ways 3d printing is changing the automotive industry," 2019.

[26] C. L. Ventola, "Medical applications for 3d printing: current and projected uses," *Pharmacy and Therapeutics*, vol. 39, no. 10, p. 704, 2014.

[27] https://www.assemblymag.com/articles/94273-additive-manufacturing-for-medical-device production, "Additive manufacturing for medical device production," 2018.

[28] https://www.dezeen.com/2016/08/30/dus-architects-3d-printed-micro-home-amsterdam-cabin bathtub/, "Dus architects builds 3d-printed micro home in amsterdam," 2016.

[29] N. Guo and M. C. Leu, "Additive manufacturing: technology, applications and research needs," *Frontiers of Mechanical Engineering*, vol. 8, no. 3, pp. 215–243, 2013.

[30] F. Chen, G. Mac, and N. Gupta, "Security features embedded in computer aided design (cad) solid models for additive manufacturing," *Materials & Design*, vol. 128, pp. 182–194, 2017.

[31] L. Sturm, C. Williams, J. Camelio, J. White, and R. Parker, "Cyber-physical vunerabilities in additive manufacturing systems," *Context*, vol. 7, no. 8, pp. 951–963, 2014.

[32] S. R. Chhetri, S. Faezi, A. Canedo, and M. A. Al Faruque, "Thermal side-channel forensics in additive manufacturing systems," in *2016 ACM/IEEE 7th International Conference on Cyber-Physical Systems (ICCPS)*, pp. 1–1, IEEE, 2016.

[33] M. A. Al Faruque, S. R. Chhetri, A. Canedo, and J. Wan, "Acoustic side-channel attacks on additive manufacturing systems," in *2016 ACM/IEEE 7th international conference on Cyber-Physical Systems (ICCPS)*, pp. 1–10, IEEE, 2016.

[34] A. Hojjati, A. Adhikari, K. Struckmann, E. Chou, T. N. Tho Nguyen, K. Madan, M. S. Winslett, C. A. Gunter, and W. P. King, "Leave your phone at the door: Side channels that reveal factory floor secrets," in *Proceedings of the 2016 ACM SIGSAC Conference on Computer and Communications Security*, pp. 883–894, 2016.

[35] S. Belikovetsky, M. Yampolskiy, J. Toh, J. Gatlin, and Y. Elovici, "dr0wned–cyber-physical attack with additive manufacturing," in *11th {USENIX} Workshop on Offensive Technologies ({WOOT} 17)*, 2017.

[36] L. D. Sturm, C. B. Williams, J. A. Camelio, J. White, and R. Parker, "Cyber-physical vulnerabilities in additive manufacturing systems: A case study attack on the. stl file with human subjects," *Journal of Manufacturing Systems*, vol. 44, pp. 154–164, 2017.

[37] T. Kurfess and W. J. Cass, "Rethinking additive manufacturing and intellectual property protection," *Research-Technology Management*, vol. 57, no. 5, pp. 35–42, 2014.

[38] O. Ivanova, A. Elliott, T. Campbell, and C. Williams, "Unclonable security features for additive manufacturing," *Additive Manufacturing*, vol. 1, pp. 24–31, 2014.

[39] K. Michael, "Autocad malware: Rare but malignant. 2013 [cited 2017 february 2nd]."

[40] C. Wei, Z. Sun, Y. Huang, and L. Li, "Embedding anti-counterfeiting features in metallic components via multiple material additive manufacturing," *Additive Manufacturing*, vol. 24, pp. 1–12, 2018.

[41] C. Harrison, R. Xiao, and S. Hudson, "Acoustic barcodes: passive, durable and inexpensive notched identification tags," in *Proceedings of the 25th annual ACM symposium on User interface software and technology*, pp. 563–568, 2012.

[42] J. Yang, H. Peng, L. Liu, and L. Lu, "3d printed perforated qr codes," *Computers & Graphics*, vol. 81, pp. 117–124, 2019.

[43] N. Gupta, F. Chen, N. G. Tsoutsos, and M. Maniatakos, "Obfuscade: Obfuscating additive manufacturing cad models against counterfeiting," in *Proceedings of the 54th Annual Design Automation Conference 2017*, pp. 1–6, 2017.

[44] F. Chen, Y. Luo, N. G. Tsoutsos, M. Maniatakos, K. Shahin, and N. Gupta, "Embedding tracking codes in additive manufactured parts for product authentication," *Advanced Engineering Materials*, vol. 21, no. 4, p. 1800495, 2019.

[45] F. Chen, J. Zabalza, P. Murray, S. Marshall, J. Yu, and N. Gupta, "Embedded product authentication codes in additive manufactured parts: Imaging and image processing for improved scan ability," *Additive Manufacturing*, vol. 35, p. 101319, 2020.

[46] F. Chen, J. H. Yu, and N. Gupta, "Obfuscation of embedded codes in additive manufactured components for product authentication," *Advanced engineering materials*, vol. 21, no. 8, p. 1900146, 2019.

[47] Y. Kubo, K. Eguchi, R. Aoki, S. Kondo, S. Azuma, and T. Indo, "Fabauth: Printed objects identification using resonant properties of their inner structures," in *Extended Abstracts of the 2019 CHI conference on human factors in computing systems*, pp. 1–6, 2019.

[48] Y. Kubo, K. Eguchi, and R. Aoki, "3d-printed object identification method using inner structure patterns configured by slicer software," in *Extended Abstracts of the 2020 CHI Conference on Human Factors in Computing Systems*, pp. 1–7, 2020.

[49] Z. Li, A. S. Rathore, C. Song, S. Wei, Y. Wang, and W. Xu, "Printracker: Fingerprinting 3d printers using commodity scanners," in *Proceedings of the 2018 ACM sigsac conference on computer and communications security*, pp. 1306–1323, 2018.

[50] M. D. Dogan, F. Faruqi, A. D. Churchill, K. Friedman, L. Cheng, S. Subramanian, and S. Mueller, "G-id: Identifying 3d prints using slicing parameters," in *Proceedings of the 2020 CHI Conference on Human Factors in Computing Systems*, pp. 1–13, 2020.

[51] R. Kikuchi, S. Yoshikawa, P. K. Jayaraman, J. Zheng, and T. Maekawa, "Embedding qr codes onto b-spline surfaces for 3d printing," *Computer-Aided Design*, vol. 102, pp. 215–223, 2018.

[52] M. Suzuki, P. Silapasuphakornwong, K. Uehira, H. Unno, and Y. Takashima, "Copyright protection for 3d printing by embedding information inside real fabricated objects.," in *VISAPP (3)*, pp. 180–185, 2015.

[53] https://en.wikipedia.org/wiki/Voronoi_diagram, "Wikipedia, the free encyclopedia - voronoi diagram."

[54] http://alexbeutel.com/webgl/voronoi.html, "Interactive voronoi diagram generator with webgl."